On the Viscosity of Liquid.

By Kunihiko KIGOSHI.

(Received October 1, 1948.)

Introduction. Up to this time, a number of theories on the viscosity of simple liquid were proposed by several authors,[1] each from a different point of view. Among these, H. Eyring's theory seems to be the most clear and general. But not in any of them was the shearing force caused by liquid viscosity made clear by the molecular kinetic theory. According to the idea of H. Eyring, the work done by shearing force on a molecule in the process of transition may be transferred to the potential energy barrier of transition of this molecule. However this approximation leaves something to be explained and it must be justified theoretically or experimentally.

The present author intends to give a theory of viscosity based on the similar idea of liquid structure used by Eyring and others. Thus the number of jumps of a molecule from one equilibrium position to the next is given by the simple formula $\nu \exp(-\omega/kT)$, where ν is the vibrational frequency of a liquid molecule, ω is a potential barrier formed by the nearest neighbour molecules, and kT, the product of Boltzmann's constant and the absolute temperature of the liquid. However, in a non-uniform flow a difference in a number of jumps between different directions may be caused not by a difference of ω, as has been usually considered, but by the directional difference of T. In this case T is not a temperature but a mean mutual kinetic energy of two molecules which effectively exerts to overcome the potential barrier. A gradient of flow and shearing force are calculated from this standpoint.

Shearing Force in a Non-Uniform Flow. Molecular arrangement in a liquid may be considered as follows. Around one molecule, Z_s nearest neighbour sites are located on a spherical shell with a radius R. Among these sites Z_m are occupied by the nearest neighbour molecules. We may neglect molecular interaction except the force f between the nearest neighbours. This force is determined by the distance between two molecules, which varies from R by the thermal motion of molecules. There exists such a force between each molecular pair, and f is the mean value of these forces. Therefore we can consider f as a function of R and θ, where θ is a variable expressing the mutual thermal motion of two molecules and we may give it the same dimension as tem-

(1) H. Eyring, *J. Chem. Phys.*, 4 (1936), 238; S. Glasstone, K. J. Laidler and H. Eyring, "The Theory of Rate Processes", 480 (1941); J. Frenkel, *Trans. Faraday Soc.*, 33 (1936), 58; S. Kaneko, This Bulletin, 15 (1940), 276.

CHEMISTRY HALL LIBRARY

perature. In general, especially in a non-uniform flow θ is a function of θ, φ which are respectively the polar coordinates of one molecule taking the other as an origin. The directional difference of θ may be small in comparison with the magnitude of θ and when we put the mean value of θ as equal to T, we may get:

$$\theta = T + \Delta\theta(\theta, \varphi) \qquad \langle \Delta\theta(\theta, \varphi) \rangle_{Av} = 0 \qquad (1)$$

where $\Delta\theta$ is a function of θ, φ and the average is taken over all possible directions. In this case f can be expressed as follows:

$$f(R, \theta) = f(R, T) + \Delta\theta \partial f / \partial T \qquad (2)$$

When the non-uniformity of a flow is expressed by a single flow gradient du/dz, were u is a flow velocity on x-direction, and the other flow gradients are zero, the consideration on the space symmetry deduces that at $\theta = 0$, $\Delta\theta = 0$, and variation of the directional variation of $\Delta\theta$ is a periodic function of θ and φ having periods π and 2π respectively. Then we may write $\Delta\theta$ in the following simple expression;

$$\Delta\theta = a \sin 2\theta \sin(\varphi + \delta) \qquad (3)$$

where a is a constant depending on du/dz and δ is a constant which will be determined in the next section.

Only the forces f between the nearest neighbours are taken into consideration, so we can easily obtain the shearing force in a liquid. If we denote by F_x the x-component of a shearing force per unit area of x, y-plane at the origin of coordinates, we may obtain F_x as a sum of x-component of the forces which act between the molecules on one side of x, y-plane (e.g. $z > 0$) and the molecules on the other side ($z < 0$). Then we may write:

$$F_x = \int_0^R \int_0^{2\pi} \int_0^{\cos^{-1}(z/R)} f(R, \theta) \sin\theta \cos\varphi \, (Z_m/4\pi) \sin\theta \, d\theta \, d\varphi \, \rho \, dz \qquad (4)$$

where ρ is the particle density of molecules in a liquid. $f(R, \theta) \sin\theta \cos\varphi$ is x-component of a force f between a molecular pair having the distance R and direction θ, φ. $(Z_m/4\pi) \sin\theta \, d\theta \, d\varphi \, \rho \, dz$ is the number of molecular pairs which have one of pair having a coordinate z between z and $z+dz$ and the other one having the direction θ, φ respectively in the small region $(\theta, \theta+d\theta)$ and $(\varphi, \varphi+d\varphi)$. The value of θ is restricted within $0 \leq \theta < \cos^{-1}(z/R)$ by the condition that one has a coordinate $z \leq 0$ and the other $z > 0$.

The pressure P in a liquid may be considered as a z-component of a force per unit area of x, y-plane acting on one side of the plane by molecules in the other side of the plane. Then in the same manner as

above we may obtain the formula for P, but this time we have to take into consideration the kinetic pressure NkT/V.

$$P = NkT/V + \int_0^R \int_0^{2\pi} \int_0^{\cos^{-1}(z/R)} f(R, \theta) \cos\theta \, (Z_m/4\pi) \sin\theta \, d\theta \, d\varphi \, \rho \, dz$$

Where V is molar volume; N, Avogadro's number, and $f\cos\theta$ is z-component of a force f. The same result may be obtained by the use of the virial theorem. This integral is easily performed with the aid of equations (2) and (3). It is obvious that the result obtained is independent of a, i. e. of gradient of flow.

$$P = NkT/V + (1/6)\, Z_m \rho \, Rf(R, T) \qquad (5)$$

In the actual case, distance R and number Z_m of the nearest neighbour depend on V and T in a complicated manner, but the approximation that R and Z_m explicitly depend only on V may be allowed in a simple liquid model. By this assumption we can obtain $\partial f/\partial T$ in equation (2) by differentiation (5) with respect to T.

$$\partial f/\partial T = (6/Z_m \rho R)\, [(\partial P/\partial T)_V - Nk/V] \qquad (6)$$

The integration of equation (4) is performed by equations (2) and (3), and referring to equation (6) the next result is obtained:

$$F_c = (2a/5)\, [(\partial P/\partial T)_V - Nk/V] \qquad (7)$$

where a constant δ is substituted by $\pi/2$ as we shall see in the next section.

The Gradient of the Flow Velocity. The molecular motion in a liquid may be considered as jumps of a molecule from one equilibrium point to another. The simplest assumption we can make is that the distance of a jump is equal to R, since a molecule jumps to any one of its nearest neighbour sites. When one molecule changes its site, it is naturally expected that some of its neighbouring molecules may change their sites at almost the same time, therefore we cannot make clear the idea of the equilibrium site of a molecule. On the contrary, the change in direction θ, φ or distance R of two molecules is the evidence of a jump of a molecule.

We suppose that a molecule A is situated at the origin and the polar coordinates of molecule B are at first R, θ, φ respectively. Now we consider a jump of molecule B which changes θ, φ to θ', φ' but keeps R constant. Molecules which hinder this kind of transition are A and some of the other nearest neighbours of B molecule. These other molecules besides A, might jump in the process of transition of B molecule. A detailed discussion about the motion of these molecules is very dif-

ficult. But we can say that the potential barrier formed by these molecules is fixed to the molecule A, i. e. to the origin of the coordinates. The probability that the molecule B passes over this potential barrier will be given by $\lambda \exp(-\omega/k\theta)$ where ω is the height of this barrier and θ is a quantity having a dimension of temperature which represents the thermal motion of B with respect to A as mentioned in the preceding section. A constant λ may be determined as follows. The consideration on the uniform state i. e. $\theta = T$, may be allowed now. In this case the probability of jumps of a molecule may be proportional to the number of available sites around this molecule. Therefore the probability of jumps of a molecule in any direction may be proportional to the number of the nearest neighbour sites Z_g, but the probability of jumps mentioned above i. e. the jumps of B to the nearest neighbour sites of A may be proportional to the number of the nearest neighbour sites common to A and B. If we denote by Z_c this number of sites, we may write these proportional relations in the following manner.

$$\nu \exp(-\omega/kT) / \lambda \exp(-\omega/kT) = Z_g/Z_c$$

Therefore $$\lambda = \nu Z_c/Z_g$$

The numerator of the left side of the above equation implies a probability of jumps in any direction as given by Simha.[2] Now we can obtain a number of jumps of B per unit time which changes θ, φ to θ', φ' but keeps R, the distance from A, constant.

$$(\nu Z_c/Z_g) \exp(-\omega/k\theta) \qquad (8)$$

Suppose there is a spherical shell with a radius R around one molecule in a liquid. We consider the conservation of the number of molecules on the small area $R^2\,dw$ on this sphere, which is intercepted by the small solid angle dw drawn at the center and directed to θ_1, φ_1. The molecules on the area $R^2\,dw$ jump away from this area by two processes, one changing only the coordinates θ_1, φ_1 and keeping R constant, the other changing R. At first we consider the latter process and its reverse i. e. jumping-in-process. These processes are the change in position of the molecules taking place on and outside of the sphere, therefore the net rate of increase of molecules on the area $R^2\,dw$ in these processes may be written as follows:

$$\rho(du/dz) R \cos\theta_1 \sin\theta_1 \cos\varphi_1 R^2\,dw \qquad (9)$$

where $(du/dz) R \cos\theta_1$ is a flow velocity in the x-direction in the small area $R^2\,dw$, and $\sin\theta_1 \cos\varphi_1 R^2\,dw$ is an area projected to the y, z-plane. On the other hand jumps of the former case and its reverse process are

(2) R. Simha, *J. Chem. Phys.*, 7 (1938), 202.

changes of molecules on the same sphere. The number of molecules jumping away from the area $R^2\,dw$ per unit time by the change of θ_1, φ_1 is expressed in a product of $\nu(Z_c/Z_j)\exp(-\omega/k\theta_1)$ and $(Z_m/4\pi)\,dw$, which is equal to the number of molecules in this area, where θ_1 means $\theta(\theta_1, \varphi_1)$. The reverse processes bring molecules to the area $R^2\,dw$ from the small circle k on the spherical shell around A. The center and the radius of this circle are respectively the small area $R^2\,dw$ and R. The number of molecules brought in by this process per unit time may be given by the product of the averaged value of (8) around the circle k and $(Z_m/4\pi)\,dw$. Therefore the net rate of increase per unit time in these two processes are

$$\nu(Z_c/Z_j)\,[\langle\exp(-\omega/k\theta)\rangle_{Av}-\exp(-\omega/k\theta_1)]\,(Z_m/4\pi)\,dw \qquad (10)$$

The sum of the expressions (9) and (10) is the total increase of molecules in the small area $R^2\,dw$ by any sort of jumps, therefore this must be zero and we obtain

$$\cos\theta_1\sin\theta_1\cos\varphi_1\,(du/dz) = (\nu Z_m Z_c/4\pi\rho R Z_j)\,(\exp(-\omega/k\theta_1) - \langle\exp(-\omega/k\theta)\rangle_{Av}) \qquad (11)$$

Then, using equations (1) and (3) we can write

$$\exp(-\omega/k\theta_1)-\langle\exp(-\omega/k\theta)\rangle_{Av} = (a\omega/kT^2)\,[\sin 2\theta_1\sin(\varphi_1+\delta) - \langle\sin 2\theta\sin(\varphi+\delta)\rangle_{Av}]\exp(-\omega/kT) \qquad (12)$$

When θ, φ are the coordinates of a point on the circle k and φ' is a parameter illustrated by Fig. 1. The calculation of the last term is performed by spherical trigonometry and we can obtain the following result.

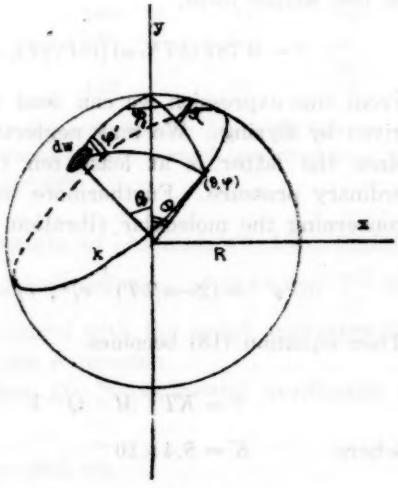

Fig. 1

$$\langle\sin 2\theta\sin(\varphi+\delta)\rangle_{Av} = \frac{1}{2\pi}\int_0^{2\pi}\sin 2\theta\sin(\varphi+\delta)\,d\varphi' = \frac{1}{8}\sin 2\theta_1\sin(\varphi_1+\delta) \qquad (13)$$

Referring to equations (12) and (13), equation (11) i. e. the condition for a number of molecules in the small area $R^2 dw$ is constant, leads to the relation between α and du/dz, and at the same time, value of the constant δ is obtained.

$$du/dz = (9\alpha Z_m Z_c \nu\omega/16\pi\rho R^3 Z_g kT^2) \exp(-\omega/kT) \tag{14}$$
$$\delta = \pi/2$$

The Expression for the Viscosity Coefficient. If we denote by η the viscosity coefficient of a liquid, the shearing force F_x in equation (5) is equal to $\eta\, du/dz$. Then equations (7) and (14) lead the expression for η.

$$\eta = (32\pi\rho R^3 Z_g kT^2/45 Z_m Z_c \nu\omega)\,[(\partial P/\partial T)_v - Nk/V] \exp(\omega/kT) \tag{15}$$

We may consider Z_m/Z_g as the ratio of the number of occupied sites to that of total sites. In the case of approximation for the face-centered cubic lattice,

$$Z_g = 12, \quad Z_c = 4 \tag{16}$$

and the value for Z_m may be put at 10 without great error. When we use the density of lattice point $2^{\frac{1}{2}}/R^3$ for the density of total sites, then the density of molecules is given as follows:

$$\rho = 2^{\frac{1}{2}} Z_m/R^3 Z_g \tag{17}$$

By these relations expression (15) may be reduced to the following more or less simple form,

$$\eta = 0.787\,(kT^2/\nu\omega)\,[(\partial P/\partial T)_v - Nk/V] \exp(\omega/kT) \tag{18}$$

From this expression we can lead a formula which is quite alike that given by Eyring. We may neglect Nk/V when compared with $(\partial P/\partial T)_v$, since the latter is at least ten times larger than the former at an ordinary pressure. Furthermore we adopt the next well-known formulas concerning the molecular vibration ν and free volume v_f.[3]

$$\nu^{-1} = (2\pi m/kT)^{\frac{1}{2}} v_f^{\frac{1}{3}}, \quad v_f = N^{-1} V^{-2} [2R/(\partial P/\partial T)_v]^3 \tag{19}$$

Then equation (18) becomes

$$\eta = KT^{\frac{5}{2}} M^{\frac{1}{3}} Q^{-1} V^{-\frac{2}{3}} \exp(Q/RT) \tag{20}$$

where $K = 8.4 \times 10^{-4}$ R = gas constant, cal/mol. deg.

(3) H. Eyring and J. Hirschfelder, *J. Phys. Chem.*, 41 (1937), 249.

M = molecular weight, V = molar volume, cm^3.
Q = activation energy for jumps, cal/mol.

Expression (20) obtained by the author differs somewhat from that of Eyring', namely, the latter has the term of heat of vaporization L_v instead of Q in the denominator of (20), i. e. it has a factor $(Q/L_v)K$ instead of K in equation (20). This difference has resulted from the different views on the relation between the flow and transition probability of a molecule. We may discuss the relative value of K of different liquids with a considerable degree of accuracy in spite of rough approximation as equation (19). The constancy of the value K for different liquids, especially in metalic liquids, each having a different and proper value of L_v/Q, is shown in Table 1. In this table the values of

Table 1.

	$\eta_m \times 10^3$	Q	L_v	L_v/Q	$K \times 10^4$
Na	7.9	0.96	25	26	5.4
K	5.5	1.15	21	18	3.8
Ag	4.4	4.87	59.5	12	3.1
Zn	33.4	2.92	24	8.2	3.7
Cd	25.3	1.59	26	16	4.0
Hg	20.1	0.598	14	23	3.9
Sn	20.3	1.603	78	49	3.5
Pb	28.5	2.32	46	20	3.2
Sb	14.6	2.92	45	16	2.0
Bi	18.6	1.715	46	27	2.7
A	2.83	0.524	1.50	2.9	1.2
N_2	3.11	0.468	1.34	2.9	1.3
O_2	8.09	0.406	1.67	4.1	3.0
CH_4	2.25	0.740	2.20	3.0	1.1
C_2H_4	7.24	0.739			3.2
CO	3.21	0.463	1.41	3.1	1.6

The values of viscosity coefficients η_m at the melting points and that of Q and L_v have been taken from Ward's table.[5] Q and L_v are given in kilocalories per gram atom or gram molecule.

Q are obtained by the simple formula of Andrade's[4] $A \exp(Q/RT)$, since we may neglect the temperature dependence of the term $T^{\frac{5}{2}} M^{\frac{1}{3}} Q^{-1} V^{-\frac{2}{3}}$ in expression (20) when compared with the rough approximation used in the course of derivation of this expression.

It may be said that Table 1 offers the experimental verification of the idea used in this paper.

(4) E. N. Da C. Andrade, *Phil. Mag.*, 17 (1934), 698.

(5) A. G. Ward, *Trans. Faraday Soc.*, 32 (1936), 88.

In conclusion the author would like to express his thanks to Dr. Y. Miyake and members of his laboratory for valuable discussions.

Meteorological Institute, Central Meteorological Observatory of Japan.

On the Barrier Layer by the Contact between the Selenium Semiconductor and Metal. II.[1]

On the Selenide Formation in the Barrier Layer.[2]

By Masao TOMURA.

(Received November 10, 1948.)

Introduction. It is well known that the barrier layer by the contact between the selenium and metal is the cause of retification and barrier layer photoeffect. The author has already explained the formation, rectification and barrier layer photoeffect of pure contact when its barrier layer consists of selenium itself.[3]

The barrier layer of a practical selenium rectifier is not of a pure contact type, but composed of selenide as pointed out by the author.[3] To improve the character of the selenium rectifier, more detailed studies on the structure of the barrier layer are desirable. Here the author will research the formation and structure of the barrier layer of a Cd-Se element.

Description of Experiments. The selenium purified by vacuum distillation is put on a base electrode in melting and it suffers a heat treatment of 4 hours at 200°C. Then cadmium is evaporated on the surface of selenium in vacuum and afterwards the cadmium film is covered with aluminium by the vacuum evaporarion to avoid tarnishing of cadmium at high temperatures.

The area of the element is 15 cm^2.

The element shows an electromotive force between the base electrode and front aluminium electrode, and it increases exponentially with temperature. Thus the current is picked up into the external circuit

(1) The previous report is in *Proc. Toshiba Lab.*, (*in Japanese*), **19** (1944), 206.

(2) Read at the annual meeting of the Phys. Soc. Jap. in Kyoto, (1948).

(3) M. Tomura, *Proc. Toshiba. Lab.*, (*in Japanese*), **18** (1943) 523; **19** (1944), 206.

and its characteristics are measured. The method of measurement is shown in Fig. 1. The current in the external circuit varies with the external resistance, so the latter is maintained as small as 25 ohms to pick up the former as much as possible. The current flows from the base electrode to the front electrode through the external circuit as shown in the figure in the same direction as the photocurrent of a selenium barrier layer photoelement. At first it amounts to about 100 micro-amperes at 100°C.

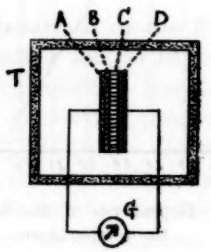

Fig. 1. Measuring apparatus.

A Al electrode.
B Cd film.
C Selenium semiconductor.
D Base electrode.
G Galvanometer.
T Thermostat.

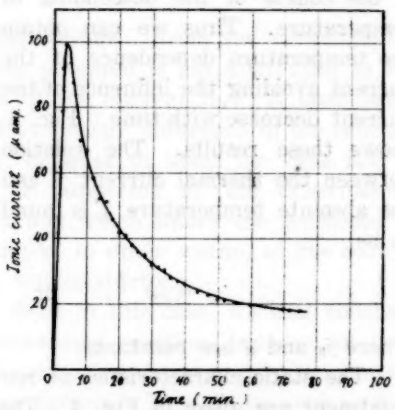

Fig. 2. Relation between the current and time

As the selenium semiconductor and both electrodes, as well as the copper lead wires, are kept at the same temperature, the current cannot be attributed to the so-called thermoelectromotive force by the temperature difference between them.

The relation between the current and time after bringing the element into the thermostat at 100°C is shown in Fig. 2. The initial steep increase of the current may mean the temperature rise of the element by its abrupt inserting into the thermostat, and the temperature of the element may reach 100°C after several minutes. Next, the current decreases with time and tends to zero asymptotically. The lower the temperature, in other words, the smaller the current, the more slowly decreases the current with time. For instance, the current does not decrease practically at room temperatures.

On the other hand, the resistance of the element becomes larger with the flow of current.

Next, the dependence of the current on the temperature is measured. As the current varies with time, cares are taken that the duration necessary to alter the temperature of the element does not influence results. Namely, the element is maintained long enough at the maximum

temperature 100°C necessary for the measurement, so that the current reaches to a practically constant value as shown in Fig. 2. And as the current becomes very small exponentially with the temperature decrease, and that makes the variation of current with time small as the above, the currents are measured in the course of the descending of temperature. Thus we can obtain the temperature dependence of the current avoiding the influence of the current decrease with time. Fig. 3. shows these results. The relation between the thermal current j and the absolute temperature T is found to be

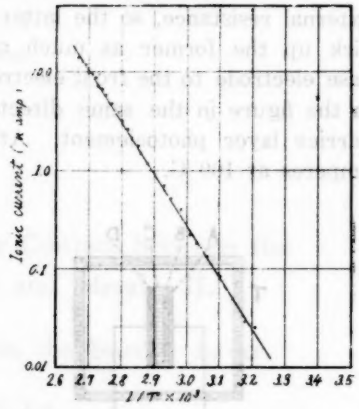

Fig. 3 Dependence of the current on the temperature.

$$j = j_0 e^{-\frac{\alpha}{T}}, \qquad \text{or} \qquad \log j = \log j_0 - \frac{\alpha}{T},$$

where j_0 and α are constants.

The static characteristics of rectification before and after the heat treatment are given in Fig. 4. The results show that the resistance of

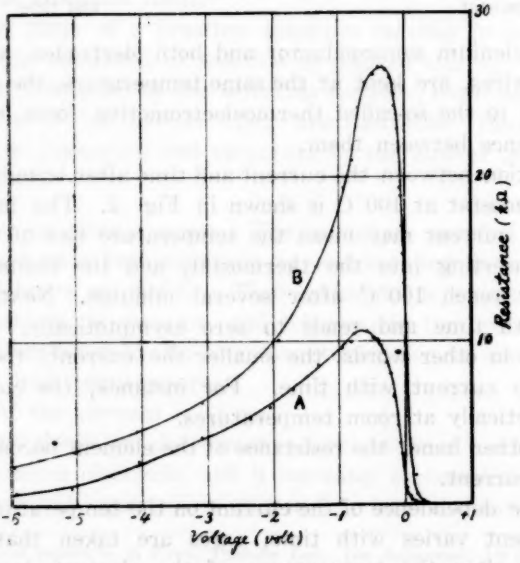

Fig. 4. Characteristics of rectification before (A) and after (B) the heat treatment of 100 min. at 100°C.

rectification of the element becomes very large by the heat treatment and furthermore the characteristics of rectification change by that treatment.

On the other hand, samples are made which have thin cadmium films of 10~50 mμ thick deposited by the vacuum evaporation on the selenium semiconductors. Their surfaces after the heat treatment of 4 hours at 210°C in vacuum are studied by the reflection method of electron diffraction. CdSe layers of the zinc blend type are observed on their surfaces.

Explanations of the Experimental Results. From the verification of the preceding section that the current observed is not attributed to any thermoelectromotive force, the cause of the current flow is none other than the converting process of the free energy difference in the reaction Cd+Se→CdSe to the electric energy, in order to keep the first law of thermodyndmics. This assumption is supported by the experimental result obtained by the electron diffraction which shows the existence of CdSe layer on the surface of the sample, in other words, at the contact of the cadmium metal and selenium semiconductor.

From the fact that the current flows in this case, we can conclude that ions move just as in the electrochemical reaction, because an ionic crystal such as CdSe shows an ionic conduction in general by the moving of ions which are derived from lattice defects. Though the ionic conduction of CdSe has not been reported, we can assume as follows: since the ionic radius of Cd^{++} is 0.60 Å, and the one of Se^{--} 1.90 Å, the defect of Frenkel type is expected for CdSe and ionic charges are carried by the moving of cadmium ions through interstitial places of the lattice.

Since there exists an internal field of the order of 10^5 v./cm. at the contact of a Cd-Se element,[3] the cause of the ionic current is that if a CdSe layer is formed by the direct reaction at the interface at first, the internal field acts upon that layer, making the cadmium ions at the interstitial points move to the selenium semiconductor side by the acceleration of the field. As the interstitial cadmium ions must take a distribution of a certain value at a given temperature, they are supplied from the cadmium electrode by the ionization of cadmium atoms into cadmium ions and electrons. The former move through the CdSe layer and the latter through the external circuit towards the selenium side, forming a new layer of CdSe. Thus the ionic current of the metal ion is observed in the external circuit. As will be mentioned afterwards, the mobility and number of the interstitial cadmium ions increase exponentially with temperature, the ionic current has the same nature, satisfying the result of Fig. 3.

The thickness of the CdSe layer becomes large with the flow of ionic current, consequently the field in the CdSe layer decreases and then the

current decreases with time as shown in Fig. 2.

The change of the rectification resistance of the barrier layer by the heat treatment shown in Fig. 4. supports certainty of the formation of the CdSe layer. By the transformation the barrier layer from one of pure contact to one of CdSe, the potential barrier at the interface becomes large for positive holes to go over the barrier, making the resistance of rectification large.

And the measurement of the abnormal spectral sensibility of a selenium barrier layer cell which has suffered a heat treatment supports the above explanation from the other side.[4]

Internal Field in the Barrier Layer which has a Selenide Layer. The potential energy of an electron in the neighbourhood of the contact

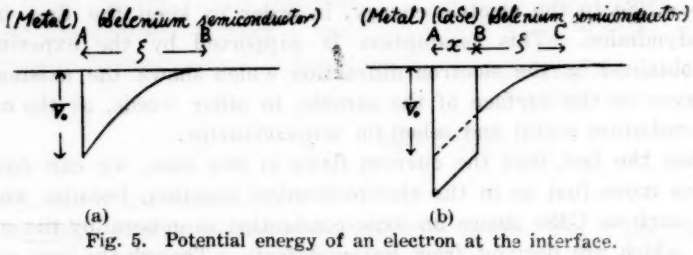

Fig. 5. Potential energy of an electron at the interface.
(a) The case of pure contact type.
(b) The case of selenide formation type.
V_0 is the contact potential difference between cadmium and selenium semiconductor.

is shown in Fig. 5. If we take N for the number of empty impurity centres in the unit volume of the selenium semiconductor and they are filled by the electrons from the metal when both elements are in contact, the potential energy of electron V is

$$\frac{d^2V}{d\xi^2} = \frac{4\pi Ne^2}{D}$$

Here e is the electronic charge and D the dielectric constant of selenium semiconductor. Then

$$\frac{dV}{d\xi} = \frac{4\pi Ne^2}{D}\xi \quad \text{and} \quad V = \frac{2\pi Ne^2}{D}\xi^2$$

are derived by taking ξ as the distance from the point B in Fig. 5 (a). If we put $1/L^2 = 2\pi Ne^2/V_0D$ into the above equations (L the thickness of the barrier layer of pure contact.), we get

$$V = \frac{V_0}{L^2}\xi^2 \quad \cdots\cdots\cdots\cdots\cdots\cdots\cdots\cdots\cdots\cdots(1)$$

(4) M. Tomura, This Bulletin, in the press.

and

$$\frac{dV}{d\xi} = \frac{2V_0}{L^2}\xi \quad \cdots\cdots(2)$$

where V_0 is the contact potential difference between both elements.

Next we take up the case in which a CdSe layer is growing. We assume that the CdSe layer is an insulator and there is no accumulation of charge at the interface between the CdSe layer and selenium. Thus if we take x as the thickness of the CdSe layer, we obtain

$$D\frac{dV}{d\xi} = D'\frac{dV}{dx} \quad \cdots\cdots(3)$$

by the continuity condition of field at the interface. Here D' is the dielectric constant of CdSe. From (2) and (3)

$$\frac{dV}{dx} = \frac{2V_0}{L^2}\frac{D}{D'}\xi \quad \cdots\cdots(4)$$

is derived. As the contact potential difference is distributed in the CdSe layer AB as well as in the selenium layer BC as shown in Fig. 5 (b), we get

$$\frac{2V_0\gamma}{L^2}\xi x + \frac{V_0}{L^2}\xi^2 = V_0,$$

namely,

$$\xi^2 + 2\gamma x\xi - L^2 = 0,$$

by considering (2) and (4), where γ is D/D'.

The solutions of the above equation are given by

$$\xi = -\gamma x \pm \sqrt{\gamma^2x^2 + L^2},$$

but from the physical standpoint we must pick up the plus sign. Thus the field $F(x)$ in the CbSe layer is

$$F(x) = \frac{dV}{dx} = \frac{2V_0\gamma}{L^2}\{\sqrt{\gamma^2x^2 + L^2} - \gamma x\} \quad \cdots\cdots(5)$$

$$= \frac{2V_0\gamma}{L^2}x\left\{\sqrt{1 + \frac{L^2}{\gamma^2x^2}} - 1\right\} \quad \cdots\cdots(5')$$

F has its maximum value $2V_0\gamma/L$ at $x = 0$ and tends to zero asymptotically with increase of x. γ may be nearly one, consequently in (5') if $L^2/\gamma^2x^2 \ll 1$, namely $x \gg L$, we get

$$F(x) = \frac{2V_0}{L^2}x\left\{\left(1+\frac{L^2}{2x^2}-\frac{L^4}{8x^4}+\cdots\right)-1\right\} \fallingdotseq \frac{V_0}{x} \quad \cdots\cdots(6)$$

and in (5) if $\gamma^2 x^2 \ll L^2$ or $x \ll L$

$$F(x) = \frac{2V_0}{L^2}(L-x). \quad \cdots\cdots(7)$$

Theoretical Calculation of the Selenide Formation. If n is the number of cadmium ions per unit volume which move through the CdSe layer and u their mean velocity, the ionic current j per unit area is given by

$$j = nu. \quad \cdots\cdots(8)$$

The charge which is brought by the cadmium ions is proportional to the formation of CdSe, that is to say, to the thickness of CdSe, so

$$jdt = a\,dx \quad \cdots\cdots(9)$$

is given, where a is a constant. The number of lattice defects n is given by

$$n = n_0 e^{-\frac{W}{2kT}} \quad \cdots\cdots(10)$$

in the case of the Frenkel type[5]. W is the energy necessary to form a lattice defect and n_0 a constant. If U is the height of the potential barrier for the travelling of ions through the lattice, u is given by the next equation,[6]

$$u = \beta e^{-\frac{U}{kT}} \sinh\left(\frac{1}{2}ZeFa/kT\right) \quad \cdots\cdots(11)$$

Here β is a constant, Z the number of electronic charge of the ion, F the field in the crystal and a the distance between the neighbouring lattice sites.

Then from (8), (9), (10) and (11), we obtain

$$j = a\frac{dx}{dt} = Ae^{-\frac{\frac{1}{2}W+U}{kT}} \sinh\left(\frac{1}{2}ZeFa/kT\right) \quad \cdots\cdots(12)$$

as the equation of growth of the selenide layer.

Here A is a constant. Since Z is 2 for a cadmium ion, a, 2.62 Å. for CdSe of the zinc blend type and kT about 0.03 e.v. at 100°C, the value

(5) e. g. N. F. Mott and R. W. Gurney, "Electronic Process in Ionic Crystals", Oxford, (1940).

(6) Ibid.

of $\frac{1}{2}ZeFa/kT$ is $10^{-1}\sim 1$, even though we consider the maximum value $2V_0/L$ of F, because V_0 is about $0.5\,v.$ and L, $10^{-5}\sim 10^{-6}$ cm.[8]

Consequently, taking up the first term of the expansion of $\sinh\left(\frac{1}{2}Ze\,Fa/kT\right)$, we can gain

$$j = a\frac{dx}{dt} = \frac{AeFa}{2kT}\, e^{-\frac{\frac{1}{2}W+U}{kT}} \qquad \cdots\cdots(13)$$

Then the relation between t and x is

$$t = \frac{2akT}{Aea}\, e^{\frac{\frac{1}{2}W+U}{kT}} \int \frac{dx}{F(x)} \qquad \cdots\cdots(14)$$

In the case of $x \gg L$, from (6) we get

$$t = \frac{2akT}{Aea}\, e^{\frac{\frac{1}{2}W+U}{kT}} \int \frac{dx}{\frac{V_0}{x}}$$

$$= \frac{akT}{Aea\,V_0}\, e^{\frac{\frac{1}{2}W+U}{kT}} x^2 + C \qquad \cdots\cdots(15)$$

where C is an integration constant. So we obtain

$$j = a\frac{dx}{dt} = \frac{AeaV_0}{2kT}\, e^{-\frac{\frac{1}{2}W+U}{kT}} \cdot \frac{1}{x} \qquad \cdots\cdots(16)$$

And if $x \ll L$, from (7) and (14) we get

$$t = \frac{2akT}{Aae}\, e^{\frac{\frac{1}{2}W+U}{kT}} \int \frac{dx}{\frac{2V_0}{L^2}(L-x)},$$

or

$$t = -\frac{akTL^2}{AaeV_0}\, e^{\frac{\frac{1}{2}W+U}{kT}} \cdot \log(L-x) + C'$$

Here C' is an integration constant and given as

$$C' = \frac{2kTL^2}{AaeV_0}\, e^{\frac{\frac{1}{2}W+U}{kT}} \cdot \log L, \text{ because } x = 0 \text{ at } t = 0.$$

Thus we obtain

$$t = \frac{akTL^2}{AaeV_0} e^{\frac{1}{2}\frac{W+U}{kT}} \cdot \log \frac{L}{L-x}, \quad \cdots\cdots(17)$$

or

$$x = L\left\{1-\exp\left(-\frac{AaeV_0}{akTL^2} e^{-\frac{1}{2}\frac{W+U}{kT}} \cdot t\right)\right\} \quad \cdots\cdots(17')$$

namely,

$$j = a\frac{dx}{dt} = \frac{AaeV_0}{kTL} e^{-\frac{1}{2}\frac{W+U}{kT}} \cdot \exp\left(-\frac{AaeV_0}{akTL^2} e^{-\frac{1}{2}\frac{W+U}{kT}} \cdot t\right) \cdots\cdots(18)$$

In Fig. 6. curves of $q\,(=\int j dt)$ versus t and q^2 versus t are plotted from the experimental data. As q is proportional to x, the curve q^2 versus t is satisfied by (15) except the region in which x is small. The

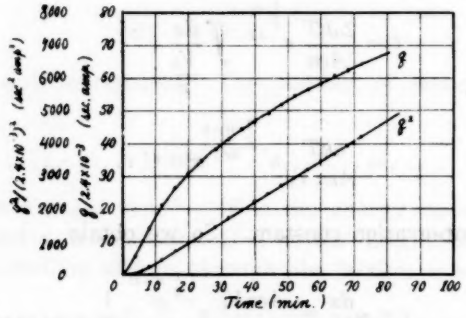

Fig. 6. q versus time and q^2 versus time curves.

region of the curve q versus t where x is small is satisfied by (17). But owing to the non-steadiness of temperature in the measurement when x or t is small, a rigorous analysis of the experimental curve in this region can not be made.

As stated above, the curve in Fig. 3 is obtained for the case in which the reaction of selenide formation progresses enough so that the CdSe layer grows thick. Then we can explain that curve by (16) which is derived for the case in which x or the thickness of the CdSe layer is large. (16) shows a linear relation between $\log j$ and $1/T$ at a given x. The activation energy of j is given as 0.98 e.v. from the experimental curve in Fig 3. and corresponds to $1/2W+U$ in (16). This value is allowable as one of a normal ionic conduction. The author has assumed that CdSe has defects of the Frenkel type, but the selection of anothor type of defects does not alter the mechanism of the selenide formation essentially.

From the presumption that the ionic current flows owing to the

internal field in the CdSe layer, (12) is substituted by

$$\sigma = \sigma_0 e^{-\frac{E}{kT}} \quad \cdots\cdots\cdots\cdots\cdots\cdots\cdots\cdots\cdots\cdots (19)$$

where σ is the ionic conductivity of CdSe and σ_0 is a constant. Assume the voltage impressed over the CdSe layer is nearly 0.5 v., because the internal field exists almost in the CdSe layer owing to the sufficient reaction in the experiment. Also assume the thickness of the layer $10^{-5}\sim 10^{-6}$ cm; σ_0 is derived as $10^3\sim 10^4$ ohm^{-1} cm^{-1}. from the experimental data in Fig. 3. This value is allowable for the moving of ions through an ionic crystal of the Frenkel type. From this magnitude of σ_0, it can be concluded that the reaction takes place at the entire area of the interface and the ions do not move through only cracks of the crystal.

As a cadmium ion transports 2 electronic charges, the thickness of the CdSe layer estimated from the value of q at 60 min. in Fig. 6 is in the order of 10^{-6} cm., considering the layer is uniform. This value is also probable for the case of heat treatment of one hour at 100°C.

Conclusion. The author found that a contact element of Cd-Se at elevated temperature had an electromotive force and the current caused by it was ionic, being attributed to the moving of cadmium ion through the CdSe layer accelerated by the internal field in the barrier layer to react with selenium.

Next the internal field in the barrier layer was calculated when the selenide formation took place and the experimental results were explained by the theoretical calculations of the formation of the CdSe layer at the contact.

Lastly, it must be pointed out that the selenide formation has an important rôle in the process of the third heat treatment in making a selenium rectifier.

The author thanks Mr. A. Otake for his co-operation in the setting of measuring apparatus.

The Matsuda Research Laboratory of
The Tokyo Shibaura Electric Co., Ltd.

On the Diamagnetism of Perylene. I.

By Haruo SHIBA and Genjiro HAZATO.

(Received November 11, 1948.)

S. Banerjee[1] has measured the principal diamagnetic anisotropies along the three principal axes on various aromatic crystals. The diamagnetic value of the perylene crystal can be found in his paper, and this may be the only experimental one which we can see in the literature on this substance before the World War II. According to his result, the mean value of the three principal susceptibilities per mole of perylene becomes -159.6×10^{-6}. It is interesting that not only does this value deviate widely from Pascal's additive law, but also, as Banerjee had already pointed out, the diamagnetic anisotropy of this molecule is almost the same in magnitude with that of pyrene. As there are some other questionable points in this problem and as we fortunately had a specimen of perylene at hand, this mesurement was newly attempted during the War. The result obtained by us showed somewhat larger diamagnetism than that of Banerjee's, and one of the values has already been published in another place briefly[2]. During the preparation of this paper, we have found in Chemical Abstracts the experimental value of this substance, reported by Pacault[3] to be $\chi_M=-165.0\times10^{-6}$, where χ_M denotes mole susceptibility.

Synthesis of the Specimen and its Purification. The perylene used in this experiment had been prepared by the method of Hansgirg and Zinke[4] by Prof. Kazuya Murata at Hiroshima Technical College, to whom we owe very much. It had been recrystallized alternatively from benzene and glacial acetic acid four times, and directly before the measurement, it was recrystallized once more from glacial acetic acid. Its melting point was 264°–265°. A part of this sample sent to Zinke had been appreciated by him to be very pure.

Magnetic Measurements. We employed the apparatus of modified type of zero point method of Weiß und Foëx[5], applying the constant field strength of about 6,000 gauß. The mass susceptibility of powdered naphthalene which had been purified by several recrystallizations and

(1) S. Banerjee, *Z. Krist.*, 100 (1939), 316.
(2) G. Hazato, *Kagaku* (*Iwanami*), 14 (1944), 162, Table 3.
(3) A. Pacault, *Ann. chim.* [12], 1 (1946), 527; cf, *Chem. Abstracts*, 42 (1948), 4409.
(4) F. Hansgirg and A. Zinke, *Monatsh.*, 40 (1919), 403.
(5) Refer, for example, to W. Klemm, "Magnetochemie," p. 46, Leipzig (1936).

sublimations, and that of purified water were chosen as standards, assuming their values to be -0.717×10^{-6} and -0.720×10^{-6}, respectively. The principle of this method lies in comparing the repulsive force, induced by the constant magnetic field in each gram of the specimen, with that of the standard substance, assuming the proportionality between the mass susceptibility and the corresponding repulsive force.[5] Both naphthalene and specimen were powdered as fine as possible, and about 0.3 g. of each of them was crammed into the globular part of quartz vessel A, which is shown in Fig. 1. The vessel A is jointed to the end of the quartz tube B held horizontally by two bifilar suspensions[5], and P shows the poles of the magnet. When A is connected to B, the two projections situated at each end of A and B are adjusted so as to be in contact with each other at the same position. In this manner, we can always reproduce the same relative position of the sample to the magnetic poles.

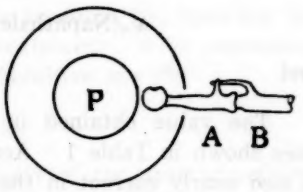

Fig. 1.

The repulsive force mentioned above can be measured by the magnitude of the counter force applied against the repulsive one so as to bring back the specimen to the original zero point by means of a weak direct current passed through the secondary coil which is situated at the other end of the quartz tube B[6]. The reading of the microammeter inserted in the circuit of the secondary coil ought to be proportional to the repulsive force, namely the product of the mass susceptibility and the weight of the sample.

The results obtained are as follows:

Table 1.

	Substance	Weight of Substance (g.)	Reading of Ammeter (μA.)	$-\chi_g\times10^6$	$-\chi_M\times10^6$
(a)	Water	0.4326	24.8	0.720 (standard)	
	Perylene	0.3530	19.0	0.676 (obtained)	170.4
(b)	Naphthalene	0.3136	17.7	0.717 (standard)	
	Perylene	0.3530	19.0	0.684 (obtained)	172.4

where χ_g and χ_M denote the mass and mole susceptibilities respectively.

Brief Considerations. If the configuration of perylene is considered to consist of two naphthalene nuclei combined at both the peri-positions, the magnetic susceptibility of this molecule may be calculated from that of naphthalene as follows:

$$\chi_M(\text{Perylene}) = 2\chi_M(\text{Naphthalene}) - 4\chi(\text{H})$$
$$= -171.8 \times 10^{-6}, \quad (1)$$

assuming that,

$$\chi_M(\text{Naphthalene})^{(6)} = -91.77 \times 10^{-6}$$

and

$$\chi(\text{H})^{(7)} = -2.93 \times 10^{-6}.$$

The value obtained in (1) coincides closely with our experimental ones shown in Table 1. Accordingly, we can say that the additive law is also nearly correct in the case of perylene, if we neglect the so-called "constitutive corrections for the trinuclear and the binuclear carbons" with regard to the central hexagon. This result shows that in perylene molecule the two naphthalene nuclei are playing a predominant role, and the central nucleus (C in Fig. 2) seems to have a special structure, having no correction term to be added for its own sake. If it were not so, the correction terms for the trinuclear carbons and for the binuclear ones would have to be added according to Pascal's additive law[7]. If these corrections were added, the resulting value would become -185.2×10^{-6}, which lies far from the experimental one. As a matter of fact, however, it is natural to consider that the origin of the correction terms for "the trinuclear and binuclear carbons" may rather be ascribed to the conditions of the planar structure of the molecular orbits in aromatic network, than to the specific character of individual carbon atom.

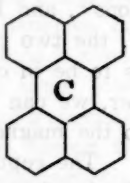

Fig. 2

On the other hand, it can be considered that aromatic molecule, in general, consists of two parts of diamagnetism, viz. the one is isotropic and the other anisotropic. The isotropic part will be represented by K_1 or K_2, showing the mole susceptibility of aromatic compounds when the molecular plane is situated parallel to the directions of the magnetic field; in this condition the anisotropic part vanishes. Let the anisotropic part per mole be ΔK, the following relationship will be satisfied,[8]

$$\Delta K = K_3 - K_1.$$

Here, K_3 represents the susceptibility when the molecular planes are put perpendicular to the direction of the magnetic field. Then in the case

(6) International Critical Tables.

(7) Cf., for instance, S. S. Bhatnagar and K. N. Mathur, "Physical Principles and Applications of Magnetochemistry," p. 90-92, London (1935); W. Klemm, "Magnetochemie," p. 160-161.

(8) L. Pauling, *J. Chem. Phys.*, 4 (1936), 676.

of fine powdered crystals, the mean susceptibility per mole becomes

$$\chi_M = K_1 + \frac{1}{3}\Delta K, \tag{2}$$

because of the planar structure of the molecule.

Accordingly, we can deduce ΔK from the equation (2), knowing the numerical value of K_1. To evaluate K_1 approximately, it is convenient to use the following modification of Pascal's additive law :[9]

$$K_1 = \sum\chi(\mathrm{C}=) + \sum\chi(\mathrm{H}), \tag{3}$$

where, $\chi(\mathrm{C}=)$ denotes the atomic susceptibility of the unsaturated carbon including the constitutive correction of half a double bond; the numerical values are[7]

$$\left.\begin{aligned} \chi(\mathrm{C}=) &= \chi(\mathrm{C}) + \frac{1}{4}\lambda(\mathrm{C}=\mathrm{C}-\mathrm{C}=\mathrm{C}) \\ &= \left(-6 + \frac{1}{4}\times 10.56\right)\times 10^{-6} = -3.36\times 10^{-6} \\ \chi(\mathrm{H}) &= -2.93\times 10^{-6}. \end{aligned}\right\} \tag{4}$$

Applying these values in (3) and (2) in combination with the experimental values of χ_M, we can calculate ΔK for various aromatic molecules. Taking the value of ΔK of benzene as the unit, we can evaluate the relative anisotropies of various aromatic hydrocarbons, the results being summarized in Table 2 together with those by other authors[10][11]

Table 2.

Substance	$-\chi_M\times 10^6$	Relative Anisotropies		
		Obs. (powd.)	Obs. (s.c.)[10]	Theo. (L.)[11]
Benzene	55.1	1	1	1
Naphthalene	91.8	2.0	2.11	2.18
Anthracene	129.2	3.05	3.38	3.45
Phenanthrene	127.9	2.97	3.07	3.19
Pyrene	147.9	3.74	4.31	4.46
Diphenyl	104.9	2.0	2.20	2.21

Here, Obs. (powd.) indicates the results obtained in the present case, and χ_M the experimental susceptibilities of powdered crystals or liquid obtained by Pascal. Obs. (s. c.) shows the results obtained by Lonsdale and Krishnan on the single crystals except in the case of benzene. Theo. (L.) shows the pure theoretical ones obtained by London.

(9) G. Hazato, *J. Chem. Soc. Japan*, **64** (1943), 483.
(10) K. Lonsdale and K. S. Krishnan, *Proc. Roy. Soc. (London)*, **A, 156** (1936), 597.
(11) F. London, *J. de Physique*, 8 (1937), 397; *J. Chem. Phys.*, 5 (1937), 837.

In the analogous manner, we can deduce the relative anisotropy of perylene to naphthalene from the results of Table 1, i. e.

$$\Delta K \text{ (Perylene)}/\Delta K \text{ (Naphthalene)} = 1.96-2.02. \qquad (5)$$

This result coincides well with that of the relation (1). The relative anisotropic values shown in Table 2 correspond approximately with the number of benzene nuclei. And from this result it may analogously be deduced that ΔK of perylene is rather 2.5 times that of naphthalene, but contrary to the supposition, the result of observation indicates as if two naphthalene nuclei predominated in the perylene molecule. If the ΔK of perylene were 2.5 times as large as that of naphthalene, $-\chi_M \times 10^6$ of perylene would be 187, which deviates widely from the experimental one.

In spite of the above mentioned discussions, there still remain many questions which we have to discuss further in detail. It may be certain, however, that from the structural point of view, the perylene molecule has essentially two predominant naphthalene nuclei, of which both the peri-bonds are somewhat longer than that of the carbon bond in benzene nucleus, but are not pure single bonds. This argument will prove to be correct, if the theoretical treatment of London[10] is modified a little. Details of it will be mentioned in the following articles.

Summary.

The diamagnetic susceptibility of perylene in powdered form has been measured and found to be $-(171 \pm 1) \times 10^{-6}$ per mole, and from this value the structure of perylene is discussed. A simple method has also been proposed to evaluate the anisotropic part from the mean molecular susceptibilities of aromatic molecules. The present result shows that perylene molecule has two predominant naphthalene nuclei and the central hexagon in this molecule has a special structure as compared with the other four.

The present writers wish to express their sincere thanks to Prof. H. Tominaga, Director of the Institute, for his kind advice and encouragement throughout this investigation. These experiments have been realized by "the Bounty for Natural Science in 1943" afforded by the Ministry of Education to one (H. S.) of the writers.

Department of Chemical Industry, Hiroshima Technical College, Hiroshima,
and
Glass Research Institute, Tohoku University, Sendai.

Flame Length and its Heat Radiation.

By Sakae YAGI.

(Recived November 16, 1948.)

This contribution involves our studies on flames during these ten years: Studies on Luminous Flames[1], Studies on Turbulent Diffusion (Flame Length)[2], and Studies on Flame Radiation[3]. In spite of wide application of flames for heating both in industrial and scientific purposes, few studies had been published particularly for design use.

The burner used in our measurement of flame length and radiation is shown in Fig. 1. Fuel gas compressed in a tank is flowed through a stream straighner and lighted at a burner nozzle, whose opening or diameter can be changed from 1 mm. to 10 mm.

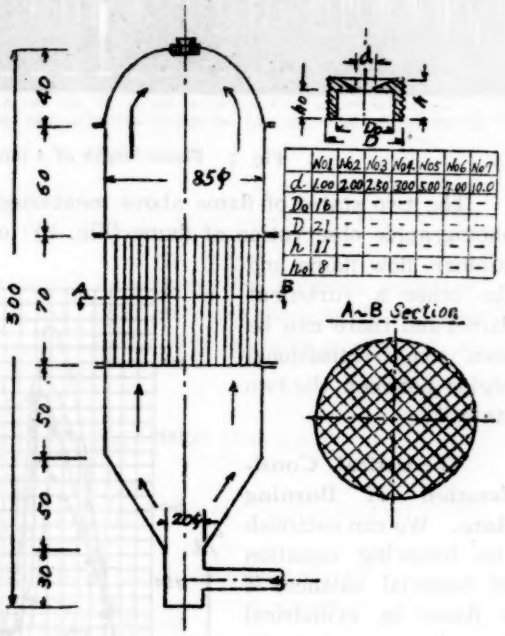

Fig. 1. Burner for measurement.

Measurement of Flame. Length of flame is measured by the picture taken in front of a bright scale background as shown in Fig. 2. Relationship between (flame length L cm.)/(nozzle diameter d cm.) and (Fuel gas velocity at nozzle opening u cm./sec.) $\times$ (d cm.) is summarized as Fig. 3 with several sizes of nozzle diameter. At the lower value of ud, L/d increases almost proportionally to ud and at the higher ud, L/d is almost independent of ud, tending to $L/d = 50-70$.

(1) J. Soc. Chem. Ind., Japan, **1937**, 90, 93, 263.
(2) J. S. C, I. J., **1943**, 608, 821, 837.
(3) J. Chem. Soc. Japan, Ind. Ed., **52** (1949), 167.

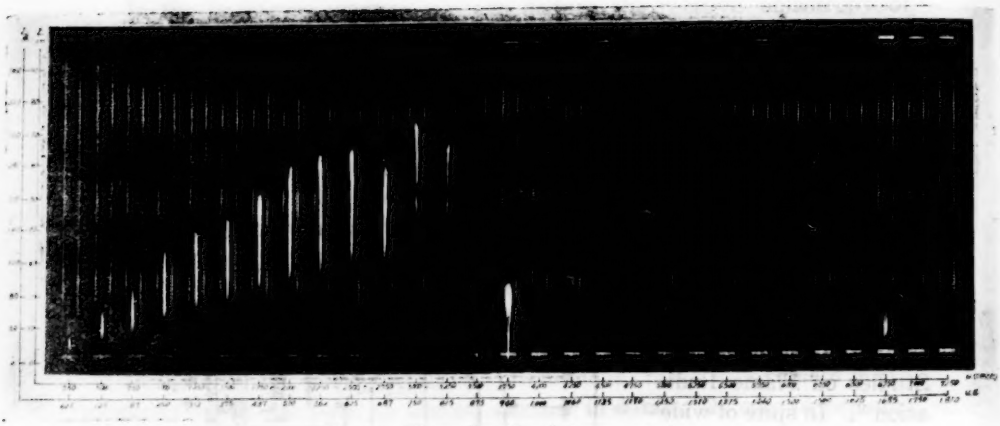

Fig. 2. Flame length of 4 mm. nozzle.

The two states of flame above mentioned are also observed by the photographic observation of flame (Fig. 2): one is a diffusional flame or laminar flow flame and the other a turbulent flame, and there can be seen some transitional region between the two states[4].

Theoretical Consideration of Burning Rate. We can establish the following equation of material balance, if a flame in cylindrical form is assumed to be mixing status of air to fuel gas by means of molecular or turbulent diffusion, which means that the chemical reaction rate of combustion is assumed to be very large compared with the mixing rate,

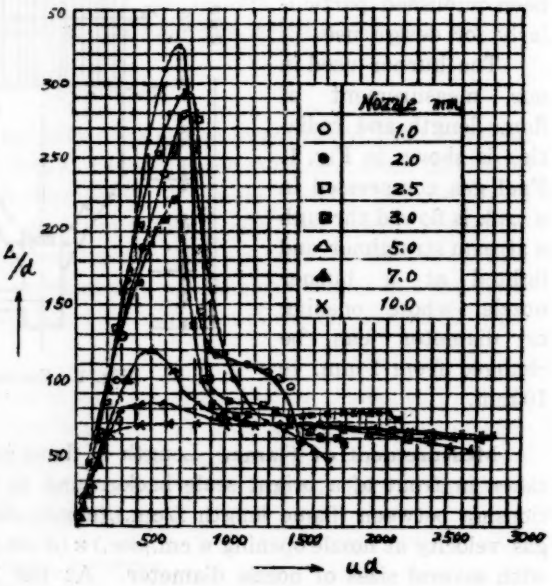

Fig. 3. Flame length.

$$\frac{\pi d^2}{4}\frac{dc}{dx}u = \pi d\frac{D+\varepsilon}{\delta}dc \quad \cdots\cdots\cdots\cdots\cdots\cdots\cdots\cdots\cdots\cdots (1)$$

(4) S. Yagi, J. S. C. I, J., **1943**, 873.

wherein d is diameter of flame, c: concentration of fuel in flame, D, ε: molecular and turbulent diffusion constant cm².sec. of air into flame through a layer length δ cm., u: velocity of flame gas cm./sec., x: length from burner nozzle. The above equation can be integrated by using average value of u, D, ϵ at the boundary condition of ordinary atmospheric combustion: $dC = C$, $C = Ci$ at $x = 0$

$$\frac{C}{Ci} = e^{-\frac{4(\bar{D}+\bar{\varepsilon})}{\bar{u}d\delta}\cdot x} = e^{-Kx} \quad \cdots\cdots(2)$$

$$K = 4(\bar{D}+\bar{\varepsilon})/\bar{u}d\delta \quad \cdots\cdots(3)$$

As the fuel concentration at the top of the flame measured was analysed as some figure like $0.1Ci$, the flame length L can be calculated by putting $C/Ci = 0.1$ and $x = L$ in equation 2.

$$\frac{L}{d} = \binom{2.3}{4}\frac{\bar{u}d\delta/d}{(\bar{D}+\bar{\varepsilon})} \quad \cdots\cdots(4)$$

$\bar{\varepsilon}$ was calculated at the jet nozzle by solving the Tollmien equation[5] as $2\times10^{-3}\, u_0 d_0$, where u_0 and d_0 are jet velocity and diameter[6]. Comparing the result of flame length measurement (Fig. 3) with equation 4, we get the following conclusions:

1. For diffusional flame:

Theoretical calculation under condition that $\bar{\varepsilon} = 0$

$$\frac{L}{d} = \binom{2.3}{4}\left(\frac{\delta/d}{\bar{D}}\right)\bar{u}d \quad \cdots\cdots(5)$$

Measured result according to nozzle diameter

$$L/d = (0.3\sim0.5)ud$$

Probable values of unknown figures

$\delta/d = 2.0\sim1.2$ changing at various d

if $D = 2.4$ cm².sec. at air diffusing through city gas at 1200°K

2. For turbulent flame at above 500 cm²./sec. of ud

Theoretical calculation under condition that $\bar{\varepsilon} = 2\times10^{-3}u_0d_0$ and $\bar{D} = 0$

$$L/d = (290)\,(\delta/d)\,u_0d_0/\bar{u}d$$

Measured average result of larger diameters

(5) Z. f. angew. Math. u. Mech., 1926, 468.
(6) S. Yagi, J. S. C. I. J., 1943, 603.

$$L/d = 60 \quad \ldots\ldots\ldots\ldots\ldots\ldots\ldots\ldots\ldots\ldots (6)$$

Probable values of unknown figures

$$(\delta/d)\,(u_0 d_0/\bar{u}d) = 0.2$$

at extreme turbulency.

3. For transitional flame:
Unable to be established definitely.

Effect of Primary Air. Although primary air in the burner frequently causes increase of combustion rate, it is not always that flame length decreases by addition of primary air as shown in Fig. 4.

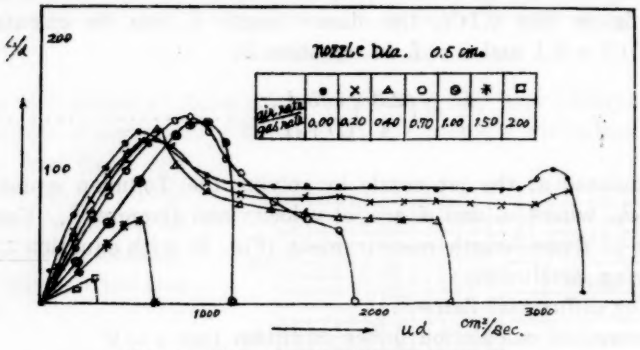

Fig. 4. Flame length adding primary air.

An important influence of adding primary air is that high primary air makes the blow limit of the gas burner have a smaller amount of ud, that means decrease in the capacity of the burner.

Further description and discussions will be available in "Flame Length III"[7].

Radiant Heat from Flame. The radiation from the flame of the above mentioned burner was measured along the length of the flame by a sensitive thermopile and galvanometer, which was calibrated with a standard black body furnace. The results measured are shown in Fig. 5, where Q_f is flame radiation integrated along the whole length of the flame, V_i is gas volume nl/h. The experiment was conducted with various openings of the burner nozzle, i.e. 1, 2, 5, 7, 10, mm. and various kinds of fuel gas, i.e.

I: City gas only of 3000 Kcal./nm.^{3},

II: City gas added with C_2H_2 6 vol. %,

(7) S. Yagi and T. Kimura, J. Chem. Soc. Japan, Ind. Ed., 1949, in printing.

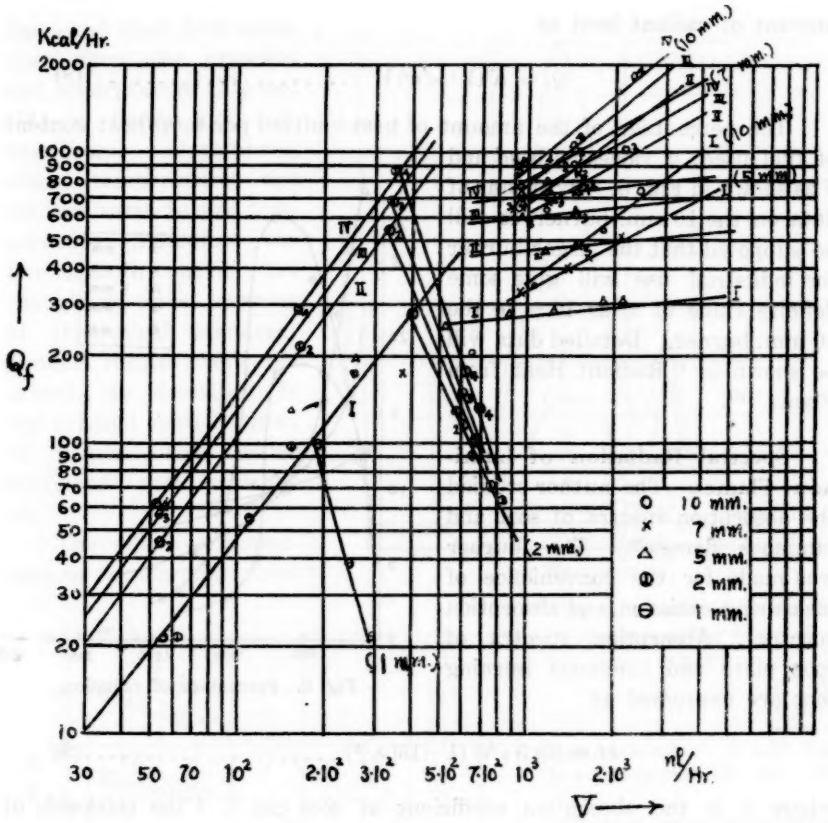

Fig. 5. Radiation from flame.

Curve I: Town Gas only.
Curve II: Town Gas plus 6 % C_2H_2.
Curve III: Town Gas plus 8 % C_2H_2.
Curve IV: Town Gas plus 10 % C_2H_2.

III: City gas added with C_2H_2 8 vol. %,
IV: City gas added with C_2H_2 10 vol. %,

In the laminar flow flame, the radiant heat Q_f is independent of burner opening, which is expressed as

$$Q_f = K(1+\alpha w)V^{1.35} \quad \ldots\ldots\ldots\ldots\ldots\ldots\ldots\ldots\ldots\ldots (7)$$

where K and α are constants, and w is the fraction of acetylene volume. In the turbulent flame Q_f decreases rapidly for smaller d and, in so far as the larger burner is concerned, Q_f is approaching the line of $Q_f = K'(1+\alpha' w)V$, which means that the industrial large burner gives such an

amount of radiant heat as

$$Q_f = K'(1+\alpha' w)V \quad \text{.....(8)}$$

The percentage of the amount of heat emitted per total heat content of fuel used, η, varies with ud and d as shown in Fig. 6. By means of data on the 10 mm. burner, it will be supposed that the larger burner for industrial use will give some definite value of η, as 10 % in the 10 mm. burner. Detailed data will be shown in "Radiant Heat from Flame"[8].

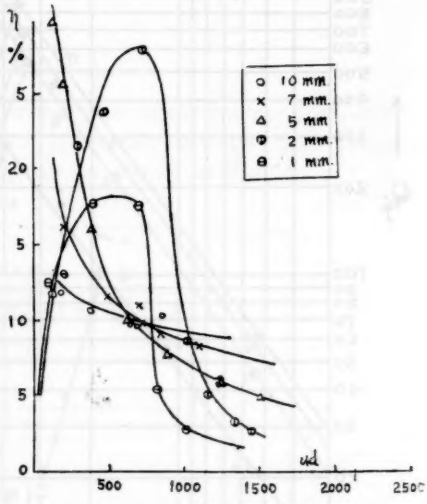

Fig. 6. Percentage of radiation.

Spectral Radiation of Luminous Flames. The author studied the absorption spectra of soot and luminous flames[9]. The burner was made for the convenience of measuring emission and absorption spectra. Absorption spectra of soot plate and luminous burning soot are expressed as

$$kl = 39.5\,\nu Nl\,(1-15[\rho\nu]^2) \quad \text{.....(9)}$$

where k is the absorption coefficient of soot cm.$^{-1}$, l the thickness of flame, ρ radius of a soot particle in μ, N number of particles in cm.^{3}, ν the wave number of spectra cm.$^{-1}\times 10^4$. The above formula was derived from the theoretical standpoint of colloidal soot particle.

The results of the experiment are shown in Fig. 7a, Fig. 7b and Fig. 8. On adding benzene vapor to city gas, spectral radiation increases as shown in Fig. 7a as I, II, III and N in equation 9 increases proportionally as shown as equations in Fig. 7b. Fig. 8 denotes flame radiation and soot radiation (thick line) and the equivalent black body radiation (thin line), of which the soot radiation was calculated from soot equations in Fig. 7b, referring to the transparent region of gas absorption, and the black body emission was calculated by dividing the emission energy with absorption data. The thin broken line shows the ideal black body emission. The differences between full and broken lines in both

(8) S. Yagi, S. Yoshida and M. Yorizane, J. Chem. Soc. Japan, Ind. Ed., 52 (1949), 167.

(9) S. Yagi, J. S. C. I. J., 1937, 90, 93, 267.

flame and black body emissions show the emission and absorption of CO_2 and H_2O in flame and surrounding atmosphere, whose temperatures are not the same as soot temperature. Therefore the two smooth curves are thought to have meaning of theoretical standard. Similar results were obtained, as described in the original contributions, in flames with added acetylene and primary air.

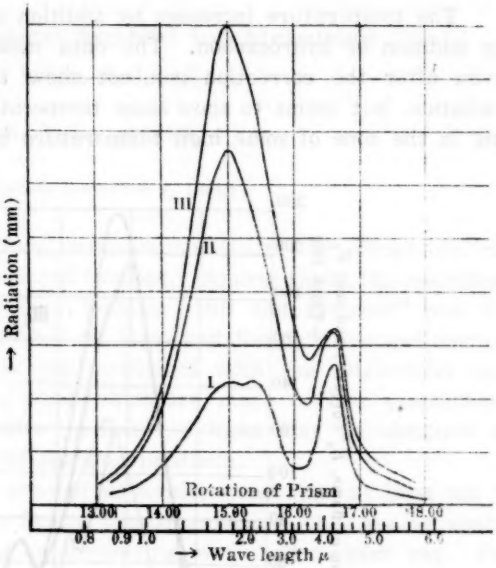

Fig. 7a. Radiation spectra of luminous adding benzene vapor

	I	II	III
		C_6H_6	
Hydrocarbon %	0	1.95	3.46
Town gas cc./mm.	144	106	100

The effective temperatures concerning heat radiation were calculated from the distribution of of black body emission as shown in the following table compared with data measured by ordinary optical pyrometer and figures corrected from absorption 650 mμ in parenthesis below.

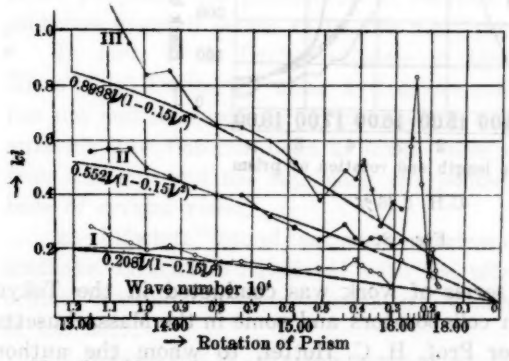

Fig. 7b. Absorption spectra of luminous flame adding benzene vapor.

Table 2. Temperatures of Several Luminous Flames.

Adding Primary Air (%)	Temp. (°C) from F′	Temp. (°C) Opt. Pyro.	Adding C_2H_2 (%)	Temp. (°C) from F′	Temp. (°C) Opt. Pyro.	Adding C_6H_6 (%)	Temp. (°C) from F′	Temp. (°C) Opt. Pyro.
0.0	1280	1370 (1450)	0.0	1360	1260 (1420)	0.0	1360	1260 (1420)
13.6	1330	1440 (1680)	3.76	1400	1400 (1515)	1.95	1260	1390 (1480)
20.8	1470	1250 (1480)	8.06	1330	1380 (1460)	3.46	1220	1320 (1440)

The temperature increases by addition of primary air and decreases by addition of hydrocarbon. The data measured by optical pyrometer even after the correction can not show the effective temperature of radiation, but seems to show some temperature of soot particles suspending in the zone of some high temperature but of relatively thin layer.

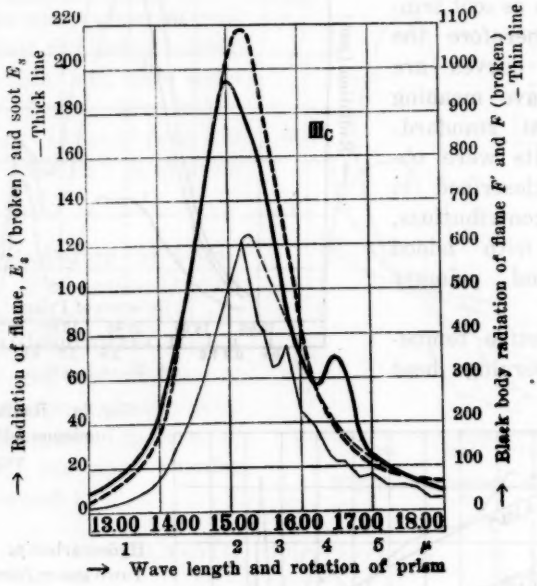

C_6H_5 3.46 %

Fig. 8.

The major part of this series of work was conducted in the Tokyo Institute of Technology with collaborators and some in the Massachusetts Institute of Technology under Prof. H. C. Hottel, to whom the author wishes to express his indebtedness.

Chemical Engineering Laboratories,
Tokyo University and Tokyo
Institute of Technology.

A New Chemical Method for Measuring the Ultra-violet Ray.

By Yasuo MIYAKE.

(Received December 1, 1948.)

1. There have been several methods to measure the ultra-violet ray using the photochemical reaction of solution. Among them, the methylene blue-acetone method contrived by Webster, Hill and Eidinow[1] and the uranyl acetate-oxalic acid method by Moss and Knapp[2] are well known. When these mixed reagents are irradiated with the ultra-violet ray, photochemical reactions take place which are more or less proportional to light energy. Thus, relative intensity of light may be obtained by quantitative determinations of reaction products.

But, as these reactions are not so sensitive and since at least ten to thirty minutes are necessary for the time of exposure, they are not useful for following a rapid change or measuring weak ultra-violet ray. For these purposes, the photochemical reaction of the leuco-base of triphenylmethane dyestuff seems to be the most promising.

In fact, I. G. Farbenindustrie in Germany offered Bioklimatische Ultra-violet Dosimeter using a colorless sulfite of fuchsin. However, it has not sufficient sensibility to measure quickly weaker radiation. The author's intention has been to make more sensitive ultra-violet radiation from the sun and the sky using the photochemical reaction of the leuco-base of crystal violet.

2. Lifschitz[3] found that when colorless cyanide or sulfite of triphenylmethane dyestuff is irradiated with the ultra-violet ray, the color of the orginal dyestuff develops immediately which gradually disappears again in the dark.

E. Weyde and W. Frankenburger[4] studied the photochemical behavior of leuco-bases of crystal violet. According to them, the rate of coloration of the leuco-base by ultra-violet ray is proportional to the quantity of light energy. The quantum yield of this photochemical reaction is almost nearly 1 in the region from 3135 Å to 2537 Å, and the maximum sensibility lies at about 2700 Å. The temperature coefficient of the reac-

(1) L. Hill, *Proc. Roy. Soc.*, **A 114** (1927), 265.

(2) Moss and Knapp, *J. Soc. Chem. Ind. Trans.*, **44** (1925), 453.

(3) Lifschitz, *Ber.*, **52** (1919), 1419; **61** (1928), 1463; Lifschitz and Joffe, *Z. physk. Chem.*, **97** (1921), 426; Lifschitz, *Z. wiss, Phot.*, **29** (1930), 91.

(4) E. Weyde and W. Frankenburger, *Trans. Faraday Soc.*, **27** (1931), 561 (The Photochemical Processes. A General Discussion.); E. Weyde, W. Frankenburger and W. Zimmermann, *Z. physik. Chem.*, **B 17** (1932), 276; *Naturwissenschaften*, **18** (1930), 206.

tion is also practically 1 in the range from $-6°$ to $+40°$C.

We have made an instrument for measuring the ultra-violet radiation using the cyanide of crystal violet as follows:

5 c.c. of the saturated solution of the leuco-base in absolute alcohol is sealed in a quartz glass ampule with an inner diameter of 13 mm. and length of 9 cm. Ten other hard glass ampules of the same size are each charged with 5 c.c. of the alcoholic solution of pure crystal violet. These are used as colorimetric standards. The concentration of the latter solution is $1.72\times10^{-5}\times(2/3)^n$ mol/litre where n is a positive integer from 0 to 9 respectively. As the solubility of the leuco-base in absolute alcohol is 5.8×10^{-5} mol/litre at room temperature, 1.72×10^{-5} mol/litre is equal to its 8/27.

We define a color standard with the concentration $n=0$ as grade 10 and successively, $n=1$ as grade 9, and so on. Measurement of light intensity is done as follows.

When an ampule containing the leuco-base solution is exposed to light for five to sixty seconds, a violet color appears. The ampule is shaken during exposure so as to mix the solution well. The time of exposure is measured with a stop watch. Then it is quickly compared with color standards protecting against the ultra-violet ray completely. When a depth of color thus attained falls between those of two color standards, the grade is read to a fractional number.

The depth of color should be proportional to the quantity of light energy received in the solution which is the product of time of exposure (t), light intensity and the surface area. Therefore, even for the same intensity of light, coloration of leuco-base solution would be different with a different time of exposure. We must reduce the coloration to that which would be obtained for a definite time exposure. Hence, we define the normal grade as a grade of color which develops when the leuco-base solution is exposed to the ultra-violet ray for just sixty seconds.

In actual cases, the time of exposure is not usually sixty seconds, so we reduce a grade of color directly observed to the normal grade to compare its light intensity with others. Let G be the normal grade, G_t, a grade obtained directly in an observation and t, time of exposure in seconds, G is calculated from the following equation.

$$G = G_t-(\log t-\log 60)/\log 3/2 \qquad (1)$$

When G is thus calculated, relative intensity of light may be easily obtained as described in the next section.

3. There is a following relation between the normal grade G and the light intensity E(erg/cm². min.)

$$\log E = \log \kappa+(G-1)\cdot\log 3/2 \qquad (2)$$

where κ is a constant depending on the wave length of light etc.

In the case of monochromatic ray, the light energy E consumed for the photochemical decomposition of the leuco-base is expressed in the following formula;

$$E = m N h \nu / s t \qquad (3)$$

where m is the number of mol of dyestuff formed; N, avogadro's number; h, Planck constant; ν, the frequency of light wave; s, the area of irradiated surface of solution, 25 cm^2.; t, time of exposure in minutes. This formula holds only in the ideal case where the quantum yield is 1 and the dark reaction is negligible. But for practical purposes, the leuco-base solution is made so as to finish the dark reaction in fifteen to thirty minutes, therefore, the rate of dark reaction can not be regarded as negligible. Moreover, the presence of impurities in reagents and the formation of a yellow decomposition product of unknown composition disturb the photochemical reaction. It is impossible to estimate these causes of error quantitatively,

The loss of light energy by reflexion and absorption may be estimated approximately as follows. According to L. Harris and J. Kaminsky[5], the rate of reflexion between the interface of the air and the quartz glass is 0.094 % at 3130 Å and at the interface between alcohol and quartz glass it is about 0.0004 %. Thus, the total depletion by reflexion is not more than about 0.09 %.

Let intensity of normal incident light be I_0, then intensity of transmitted light I is,

$$I = I_0 \times 10^{-K \cdot c \cdot d} \qquad (4)$$

where K is the absorption coefficient of the leuco-base solution, 3.16×10^{-4}; c, its concentration, 5.8×10^{-5} mol per litre; d, depth of liquid. As the solution is contained in an ampule, the depth of liquid is.

$$d = 2\{r^2 - (\alpha r)^2\}^{\frac{1}{2}} \qquad (5)$$

where r is the inner radius of an ampule, 6.5 mm.; and α is a variable between 0 at the margin and 1 at the center of the ampule. From the above formulae, we obtain approximately 1.9 % as the mean value of absorption. Therefore, it may be said that about 2 % of light energy is lost by reflexion and absorption before the formation of dyestuff begins. After the dyestuff is formed, it will act as an absorber of light, the rate of which is proportional to its concentration.

Since radiation from ordinary light sources, for example, quartz mercury lamp, the solar radiation etc., is by no means monochromatic,

(5) L. Harris and J. Kaminsky and R. G. Simard, J. Am. Chem. Soc., 57 (1935), 1151.

the light energy can not be calculated simply by the formula (3). In short, the quantitative determination of the ultra-violet ray is impossible due to complicated sources of uncertainty as explained above.

However, it may be said that only an approximate relative value of light energy can be obtained by such simple colorimetric determination of dyestuff produced by light having the same distribution of wave length. And also, at least, the mere estimation of the order of energy may be given. For instance, in the case of measuring the solar ultra-violet light intensity, the following approximate treatment can be allowed.

4. When we combine the wave length distribution curve of the solar radiation with that of the sensitivity of the leuco-base solution, an almost triangular area is obtained whose base extends from 3450 Å to 2850 Å. The wave length which divides this triangle into two equal areas is 3105 Å. Therefore, we may consider that in measuring the intensity of the ultra-violet solar radiation with our method, it may be approximately assumed without committing a great error as the monochromatic ray having the wave length of 3150 Å. When we put in the formulae (2) and (3) the value of ν corresponding to this wave length, the value of κ is obtained as follows:

$$\kappa = 0.03423 \times 10^4 \text{erg/cm.}^2, \text{ min.}$$

With the above value of κ, we can calculate the intensity of the ultra-violet ray of the sun quite approximately by multiplying E by the reciprocal of the rate of absorption (0.019), assuming that the light energy is fully used for the photochemical decomposition of leuco-base molecules. As stated avove, this is not the case, therefore the calculated value would be always smaller than the true intensity. But the relative intensity of the ultra-violet radiation of the sun can be fairly well measured by this method. It has been applied with good results to observe even the rapid change of radiation as in the case of the solar eclipse, or weaker radiation such as on a rainy day. The sensitivity and the convenience of this method are by far better than other chemical methods and comparable even tr photo-electrical tubes. But it is a weak point of this method that the sensitivity decreases gradually in the course of time.

Summary

The author has contrived a new instrument to measure the relative intensity of the ultra-violet radiation using the leuco-base of crystal violet. A quartz glass ampule containing the leuco-base solution is exposed to light and the dyestuff thus produced is determined colorimetrically with a series of a standard solution of crystal violet contained in ampules of the same size. The method of measurement is explained.

In conclusion the author expresses his thanks to Dr. Okada, the former director of the Central Meteorological Observatory of Japan for his valuable suggestions on this work.

Meteorological Institute,
Tokyo, Japan.

Étude sur la précipitation de la protéine par les sels complexes métalliques. I.

Précipitation de la protéine par les sels complexes du cobalt.

Par Réinosuké HARA.

(Reçu le 13 Décembre, 1948.)

Introduction. Quand on a l'intention d'étudier l'action du composé inorganique donné à l'organisme, on doit d'abord penser à celle sur les protéines qui constituent cet organisme. Comme beaucoup de sels inorganiques cependant se hydrolysent dans leur solution aqueuse, l'étude systématique est assez difficile. J'ai donc utilisé pour ce but les sels complexes métalliques qui ne subissent pas l'hydrolyse dans leur solution aqueuse. Récemment, Brintzinger[1] et ses collaborateurs ont determiné la constante de la dialyse des ions complexes dans la solution aqueuse, et ils ont demontré que beaucoup de sels complexes donnent leur poids moléculaire calculé par cette formule. L'étude sur la précipitation de la protéine par les sels complexes métalliques a été étudiée par S. E. Michael[2]. Il a principalment employé les sels complexes du chrome. Il a classé tous les sels complexes métalliques en sels complexes cationiques et anioniques et il a aussi démontré que le premier précipite la protéine dans le domaine alcalin du point isoélectrique et le second précipite la protéine dans le domaine acide. Comme exemples il a donné $[Cr(NH_3)_6]Cl_3$, $[Co(NH_3)_4CO_3]Cl$ pour le premier, $K_3[Cr(CNS)_6]$ pour le second. Dans ce cas, la protéine et les ions complexes peuvent réagir stoichiométriquement. J'ai déjà utilisé les sels complexes du cobalt et je vais maintenant procéder à l'expérience avec certains sels complexes typiques du fer, du chrome etc. En employant les sels complexes du cobalt, dans ce présent mémoire, je les ai classés en sel complexe cationique et sel complexe anionique comme Michael l'a déjà fait. Les solutions employées pour mes expériences montrent les *p*H 8.8 et 2, et celles du tampon sont NH_4OH-NH_4Cl à 1/10 N et $(HOOC)_2(CHOH)_2-(NaOOC)_2(CHOH)_2$ à 1/10 N.

(1) H. Brintzinger, *Z. anorg. allgem. Chem.*, **222** (1935). 312; **223** (1935). 253.
(2) S. E. Michael, *Biochem. J.* **33** (1939), 924.

Détermination du domaine de la concentration du sel complexe qui précipite la protéine. Les sels complexes cationiques ne peuvent pas toujours précipiter la protéine, tandis que les sels anioniques le font. L'alubumine d'œuf n'est guère précipitée par les sels complexes cationiques, ni la gélatine non plus. En prenant la solution de la caséine à 0.5 % ou celle de l'alubmine à 0,5 %, on les a dissous dans le tampon (*p*H 8.8 ou 2), et on a ajouté 1cc. de la solution de diverses concentrations du sel complexe à 1 cc de chaque solution. On en a examiné les résultats de précipitation après trente minutes, le résultat est montré dans la table suivante en indiquant ⧺ la précipitation parfaite, et ⧺, + la précipitation imparfaite.

a. Précipitation de la protéine par les sels complexes cationiques. Les sels complexes cationiques ne précipitent pas toujours la protéine. Aucune protéine n'est précipitée par les sels complexes du cobalt de la valence +1. Le sel complexe qui n'a pas de charge électrique tel que $[Co(NH_3)_3(NO_2)_3]$ ne précipite jamais la protéine. Le domaine de la concentration du sel complexe pour la précipitation est montré ci-dessous.

Table 1.

Sel complexe	Caséine	Insuline	Albumine d'œuf	Gélatine
$[Co(NH_3)_3(NO_2)_3]$	−	−	−	−
$[Co(NH_3)_4CO_3]_2(SO_4)\cdot 3H_2O$	−	−	−	−
$[Co(NH_3)_4(NO_2)_2^{(1)}_{(6)}]Cl$ (Trans) (Croséo)	−	−	−	−
$[Co(NH_3)_5Cl](NO_3)_2$ (Purpuréo)	+	+	−	−
$[Co(NH_3)_5NO_2]Cl_2$ (Xantho)	+	+	−	−
$[Co(NH_3)_5NO_3]Cl_2$	+	+	−	−
$[Co(NH_3)_6]Cl_3$ (Luthéo)	⧺	⧺	−	−
$[Co\,en_3]Cl_3\cdot 3H_2O$	⧺	⧺	−	−
$[Co(NH_3)_5H_2O](NO_3)_3$ (Roséo)	⧺	⧺	−	−
$[Co(NH_3)_4(H_2O)_2](No_3)_3H_2O$ (Diroséo)	⧺	⧺	−	−
$[Co(en)_2(NH_3)_2^{(1)}_{(6)}]Br_3\cdot H_2O$ (Trans)	⧺	⧺	−	−
$\left[(NH_3)_4Co\begin{matrix}OH\\OH\end{matrix}Co(NH_3)_4\right]Cl_4\cdot 4H_2O$	⧺	⧺	+	−
$\left[en_2Co\begin{matrix}OH\\OH\end{matrix}\begin{matrix}H_2O\\Co\\H_2O\end{matrix}\begin{matrix}OH\\OH\end{matrix}Co\,en_2\right]Cl_4$	⧺	⧺	+	−
$\left[Co\left(\begin{matrix}OH\\OH\end{matrix}Co\,en_2\right)_3\right](NO_3)_6\cdot 3H_2O$	⧺	⧺	+	−

Table 2.

Sel complexe	Protéine	La concentration pour la préciptation (mol)
$[Co(NH_3)_5Cl](NO_3)_2$ (Purpuréo)	Caséine	1/60
$[Co(NH_3)_6NO_2]Cl_2$	,,	1/60
$[Co(NH_3)_5NO_2]Cl_2$ (Xantho)	,,	1/40
$[Co(NH_3)_6]Cl_3$ (Luthéo)	,,	1/20—1/300
$[Co\ en_2]Cl_2 \cdot 3H_2O$	,,	1/40—1/300
$[Co(NH_3)_5H_2O](NO_3)_2$ (Roséo)	,,	1/80—1/250
$[Co(NH_3)_4(H_2O)_2](NO_3)_3 \cdot H_2O$ (Diroséo)	,,	1/40—1/250
$[Co\ en_2(NH_3)_2](Br_3 \cdot H_2O$	,,	1/40—1/300
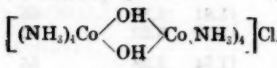	,,	1/100—1/1000
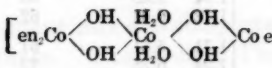	,,	1/100—1/1000
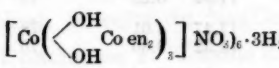	,,	1/100—1/5000

b. Précipitation de la protéine par les sels complexes anioniques. Les sels complexes anioniques peuvent parfaitement précipiter la protéine.

Table 3.

Sel complexe	Caséine	Insuline	Albumine d'œuf	Gélatine
$K[Co(NH_3)_2\ NO_2)_4]$ (Sel Erdmann)	###	###	###	+
$Na_3[Co(NO_2)_6]$	###	###	###	+
$K_3[Co(CN)_6]$	###	###	###	+

Le domaine de la concentration du sel complexe pour la précipitation est montré ci-dessous.

Table 4.

Sel complexe	Protéine	La concentration pour la précipitation (mol)
$K[Co(NH_3)_2\ NO_2)_4]$ (Sel Erdmann)	,,	1/60
$Na_3[Co\ NO_2)_6]$	,,	1/40—1/300
$K_3[Co(CN)_6]$	,,	1/100—1/300
$K[Co(NH_3)_2(NO_2)_4]$ (sel Erdmann)	Albumine d'œuf	1/60
$Na_3[Co(NO_2)_6]$	,,	1/40—1/350
$K_3[Co(CN)_6]$	,,	1/100—1/300

Calcul de l'équivalent de l'ion complexe combiné avec 1g. de la protéine. La protéine est précipitée par les sels complexes, et on peut séparer par la centrifugation en la lavant cinq fois par l'eau, et on peut la sécher dans l'exsiccateur. En prenant 20-30 mg. de la protéine précipitée et la décomposant par l'acide azotique fumant, on peut colorimétri-

quement faire le dosage du cobalt en utilisant le sel du nitroso-R[3]. Pour ce dosage du cobalt, on a d'abord calculé la quantité de l'ion complexe combinée avec 1g. de la protéine, et déterminé l'équivalent de son ion complexe.

a. Equivalents des ions complexes des sels complexes cationiques. Les équivalents des ions complexes des sels complexes cationiques sont montrés ci-dessous. (*p*H 8.8)

Table 5.

Sel complexe	Protéine	Concentration du sel complexe (mol)	Co (%)	Ion complexe (%)	Equivalent combiné avec 1g. de la protéine ($\times 10^{-5}$)
$[Co(NH_3)_5Cl](NO_3)_2$ (Purpuréo)	Caséine	1/30	1.31	5.59	65
			1.72	5.23	62
$[Co(NH_3)_5NO_3]Cl_2$	,,	,,	1.54	5.38	55
			1.72	6.01	62
$[Co(NH_3)_5NO_2]Cl_2$ (Xantho)	,,	,,	1.71	5.51	61
			1.94	6.25	70
$[Co(NH_3)_6]Cl_3$ (Luthéo)	,,	1/60	1.47	4.01	78
			1.32	3.60	70
$[Co\,en_3]Cl_3 3H_2O$	,,	,,	1.51	6.12	82
			1.44	5.83	78
$[Co(NH_3)_5H_2O](NO_3)_3$ (Roséo)	,,	,,	1.35	3.71	71
			1.41	3.87	75
$[Co(NH_3)_4(H_2O)_2](NO_3)_3 \cdot H_2O$ (Diroséo)	,,	,,	1.30	3.59	68
			1.43	3.95	76
$[Co\,en_2(NH_3)_2^{(1)}_{(6)}]Br_3 \cdot H_2O$	,,	,,	1.49	5.38	80
			1.38	4.98	74
$\left[(NH_3)_4Co\begin{matrix}OH\\OH\end{matrix}Co(NH_3)_4\right]Cl_4 \cdot 4H_2O$	,,	1/150	2.58	6.30	93
			2.39	5.83	86
$\left[en_2Co\begin{matrix}OH\\OH\end{matrix}\begin{matrix}H_2O\\Co\\H_2O\end{matrix}\begin{matrix}OH\\OH\end{matrix}Co\,en_2\right]Cl_4$	,,	,,	3.49	10.23	88
			3.60	10.60	91
$\left[Co\left(\begin{matrix}OH\\OH\end{matrix}Co\,en_2\right)_3\right](NO_3)_6 \cdot 3H_2O$	,,	5/1125	3.78	11.18	108
			3.91	11.56	112
,,	Albumine d'œuf	1/300	1.18	3.48	31
			1.62	4.79	43

Quant aux sels complexes cationiques du cobalt, les équivalents ne sont pas determinés. C'est-à-dire, l'équivalent du $\left[Co\left(\begin{matrix}OH\\OH\end{matrix}Coen_2\right)_3\right](NO_3)_6$ est 108×10^{-6}, et celui du $[Co(NH_3)_6]Cl_3$ est 78×10^{-5}, et celui du $[Co(NH_3)_5Cl](NO_3)_2$ est 65×10^{-5}. Quant aux sels complexes de la valence +2, si on répète la précipitation dans les mêmes conditions, les équivalents des ions complexes ne s'accordent pas et donnent des différences assez grandes. (plus de 10 %).

(3) H. S. van Klooster, *J. Am. Chem. Soc.*, 43 (1921), 746; F. J. Stare et C. A. Elvehjem, *J. Biol. Chem.*, 99 (1933), 473; H. T. Macpherson et J. Stewart, *Biochem. J.*, 32 1938), 763; N. Tanaka, *ce bulletin*, 18 (1943), 436.

b. Equivalents des ions complexes des sels complexes anioniques. Les équivalents des ions complexes des sels complexes anioniques sont montrés ci-dessous.

Table 6.

Sel complexe	Protéine	Concentration du sel complexe	Co (%)	Ion complexe (%)	Equivalent combiné avec 1g. de la protéine ($\times 10^{-5}$)
$K[Co(NH_3)_2(NO_2)_4]$ (Sel Erdmann)	Caséine	1/25	4.44	20.85	95
$Na_3[Co(NO_2)_6]$	,,	1/40	1.61	9.14	90
			1.58	8.97	88
$K_3[Co(CN)_6]$	,,	,,	1.72	6.27	93
$K[Co(NH_3)_2(NO_2)_4]$ (Sel Erdmann)	Albumine d'œuf	1/25	3.50	16.43	71
			3.55	16.67	72
$Na_3[Co(NO_2)_6]$	,,	1/40	1.31	7.44	72
			1.35	7.67	74
$K_3[Co(CN)_6]$	,,	,,	1.45	5.29	78

Quant aux sels complexes anioniques du cobalt, les équivalents restent constants. C'est-à-dire, l'équivalent du $K[Co(NH_3)_2(NO_2)_4]$ est 95×10^{-5} (caséine), et celui du $Na_3[Co(NO_2)_6]$ est 90×10^{-5} (caséine).

Conclusion 1. Comme S. E. Michael, j'ai classé tous les sels complexes cobaltiques en complexe cationique et complexe anionique. Le premier précipite la protéine dans le domaine alcalin du point isoélectrique et le second précipite dans le domaine acide.

2. Le sel complexe qui n'a pas de charge électrique tel que $[Co(NH_3)_3(NO_2)_3]$ ne précipite jamais la protéine.

3. Les sels complexes cationiques de cobalt ne précipitent pas toujours la protéine.

4. La précipitation de la protéine par les sels complexes cationiques du cobalt est imparfaite, et les complexes cobaltiques de la valence+1, tels que $[Co(NH_3)_4CO_3]_2SO_4 \cdot 3H_2O$, $[Co(NH_3)_4(NO_2)_2]Cl$ ne peuvent pas précipiter la protéine.

5. On peut cependant parfaitement précipiter la protéine par les complexes anioniques du cobalt.

6. Quant aux sels complexes cationiques du cobalt qui ne peuvent pas montrer la précipitation parfaite de la protéine, les équivalents ne sont pas determinés. A la même valence, ses équivalents sont approximativement identiques, tandis qu'en valence différente, ils ne sont pas identiques et diminuent proportionellement à la valence.

7. Quant aux sels complexes anioniques du cobalt, la précipitation est parfaite, et les équivalents combinés avec 1g. de la protéine restent constants independemment de la valence.

8. Les équivalents des ions complexes cationiques du cobalt combinés avec 1g. de l'albumine d'oeuf sont très petits.

9. De ces résultats, on peut conclure que la protéine et le sel complexe peuvent réagir stoichiométriquement, mais la précipitation de la

protéine par les sels complexes cationiques du cobalt n'est pas parfaite, et son équivalent de l'ion complexe combiné avec 1 g. de la protéine ne montre pas d'équivalent maximum. On peut cependant obtenir la précipitation parfaite par les sels complexes anioniques du cobalt, et son équivalent montre l'équivalent maximum.

En terminant ce compte rendu de mes recherches, j'ai à exprimer mes sincères remerciments à M. le Prof. Kénjiro Kimura pour les aimables et très utiles indications, ainsi qu'à M. M les Profs. Toshi Inoué, Taku Uémura, et Eiji Ochiai qui ont bien voulu me prêter leur bienveillant concours dans mes expériences.

Laboratoire de Chimie minérale, Faculté des Sciences, Université de Tokyo.

The Monolayer of Cresol Resin.*

By Keizô SUZUKI.

(Received December 14, 1948.)

The polymers from para-substituted phenols and formalin can make monolayers according to their linear structures.

The structure of the condensed polymer of *p*-cresol and formaldehyde is presumed chemically as

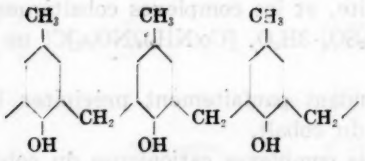

(1)

If it has actually such a structure, all OH groups in the monolayer are oriented to the water surface because of their hydrophilic nature, and the linear chain lies on the surface thrusting upwards the hydrophobic methyl groups. It is verified by experiments.

We make the monolayer by dropping the chloroformic solution of the polymer on the water and measure the relation between the surrace area and the surface pressure. The film is a condensed film. The area per phenolic radical is equal to those of *p*-alkyl phenols studied by Adam.[1] It is an evidence of the orientation of the phenolic groups on water.

---

* Read before the annual meeting of the Society on april 3, 1948

(1) N. K. Adam, "The Physics and Chemistry of Surfaces" 50, Oxford (1938).

For rigorous confirmation we measured the surface pressure of dimer, trimer, tetramer, pentamer, hexamer and heptamer:

$$(CH_3C_6H_2\underset{OH}{}CH_2)(CH_3C_6H_2\underset{OH}{}CH_2)_n(CH_3C_6H_3OH), \quad n=0, 1, 2, 3, 4, 5.$$

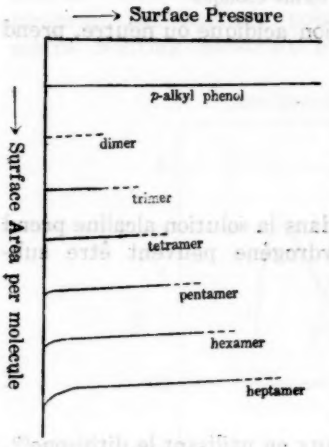

Fig. 1.

The results are shown in Fig. 1.

We can conclude that the structure of the oil-soluble phenolic resin is the linear form of (1).

The alcohol soluble polymer of phenol and formalin obtained by acidic catalysis, can never spread into monolayer. This means that the structure of the resin is quite different from that of *p*-cresol resin.

The author wishes to express his sincere thanks to Prof. J. Sameshima of Tokyo University and Prof. I. Sano of Nagoya University for their kind guidances and encouragements.

Masaoka-cho, Toyokawa, Aichi pref., Japan.

Etudes spectroscopiques des complexes métalliques du diphénylthiocarbazone. I[1].

Par Taku UEMURA et Seinosuke MIYAKAWA.

(Reçu le 19 janvier, 1949.)

Introduction. Le diphénylthiocarbazone (dithizone) donne plusieurs complexes intermoléculaires métalliques qui sont généralement solubles dans le chloroforme ou le tétrachlorure de carbone en donnant des solutions colorées foncées. On peut donc utiliser cette réaction à l'analyse qualitative et quantitaive[2]. H. Fischer[2] a déjà avancé une proposition sur l'existence de deux tautomères pour ces complexes, parce que le dithizone montre deux sortes de constitutions: soit cétonique, soit énolique, qui alternent comme ci-dessous

(1) Exposé fait lors de la 1ère Séance annuelle de la Société chimique du Japon, le 4 avril, 1948.

(2) H. Fisher, *Z. angew. Chem.*, 47 (1934), 685.

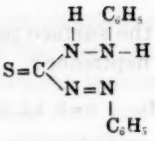

forme cétonique

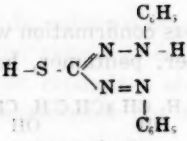

forme énolique

Le composé cétonique stabilisé dans la solution acidique ou neutre, prend la forme de

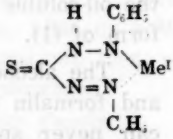

tandis que le composé énolique qui est stable dans la solution alcaline prend la constitution de laquelle deux atomes d'hydrogène peuvent être substitués par le même métal.

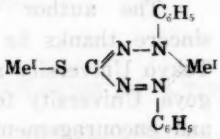

Plusieurs études sur la microanalyse des métaux en utilisant le dithizone[3], ont été déjà faites, mais les recherches spectrochimiques sur les complexes du dithizone n'étaient analytiquement poursuivies que dans la région visible[4]. Nous avons quantitativement mesuré les spectres d'absorption du dithizone et certains de ses complexes dans la région visible et ultraviolette.

Procédé expérimental. Comme le dithizone est très oxydable et qu'on peut l'obtenir au marché et qu'il est presque toujours trouvé dans ses produits oxydés, il est nécessaire de le purifier et en préparer la solution type. On dissout d'abord 20 mg. du dithizone dans 100 c.c. du tétrachlorure de carbone, puis on filtre la solution, puis on ajoute 100 c.c. d'ammoniaque de 0,2 normal et remue ce mélange. En séparant la couche du dissolvant, on y ajoute à nouveau 100 c.c. du tétrachlorure de carbone, et on acidifie le mélange par l'acide chlorhydrique. A ce moment, le dithizone se transmet de la couche aqueuse à celle du tétrachlorure de carbone. Cette solution est séparée et lavée plusieurs fois par l'eau, puis passée au filtre en papier sec pour la conserver à l'abri de la lumière. Pour déterminer la concentration du dithizone, on titre 0,01 normal de la solution d'argent nitrate par la solution du dithizone. La solution dont la concentration a été déterminée est utilisée pour mesurer ses spectres d'absorption en la diluant convenablement. L'eau, le tétrachlorure de carbone, l'ammoniaque et l'acide chlorhydrique qui sont employés pour ces expériences, sont deux fois distillés

(3) Voir les bibliographies qui se trouvent dans "Organic Reagents in Inorganic Analysis", par I. Mellan (1941), p. 96.

(4) H. A. Liebhafsky et E. H. Winslow, *J. Am. Chem. Soc.*, 59 (1937), 1966; H. Fischer et W. Weyle, *Wiss. Veröff. Siemens-Werk*, 14, II (1935), 41.

pour éviter toutes impurités qui pourraient être des causes d'erreur. Dans ces présentes études, les concentrations du dithizone et des complexes dans le tétrachlorure de carbone ou dans l'ammoniaque restent entre 2×10^{-5} et 4×10^{-5} mol/l. Nous nous sommes servis du spectrographe en quartz "type E 2" construit par Hilger et du spectrophotomètre Spekker construit par Shimazu pour la région ultraviolette. Le spectrophotomètre Nutting construit par Hilger a aussi été utilisé pour la région

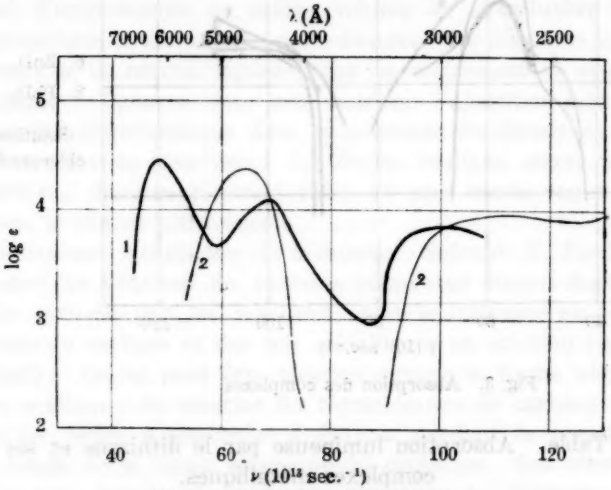

Fig. 1. Absorption du dithizone.
1. Forme cétonique (solution du tétrachlorure de carbone).
2. Forme énolique (solution ammoniaque de 0.2 normal).

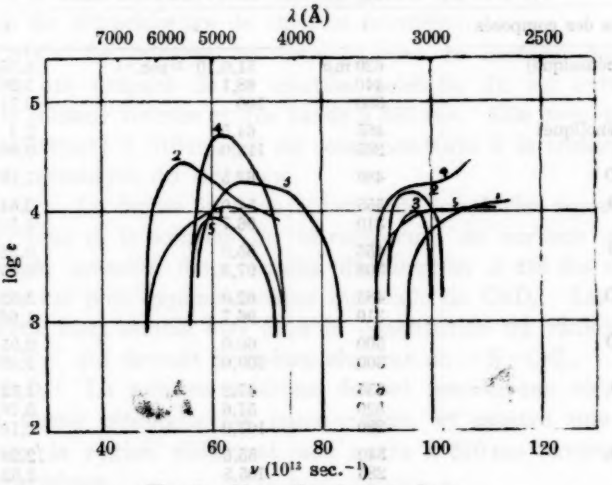

Fig. 2. Absorption des complexes.
1. AgD, 2. CuD_2. 3. CuD. 4. HgD_2. 5. HgD.
(solution du tétrachlorure de carbone).

visible. Les résultats sont indiqués dans la table suivante et par les figures 1, 2 et 3.

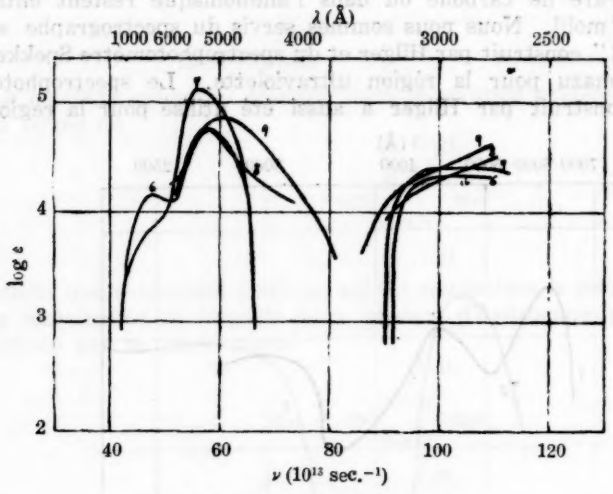

Fig. 3. Absorption des complexes.

Table. Absorption lumineuse par le dithizone et ses complexes métalliques.

ε = valeurs des coefficients d'absorption meléculaire.
D = dithizone. λ = longueur d'onde. ν = fréquence.

Formes des composés	λ	ν	ε
D (cétonique)	620 mμ	51,0.10 ^{13} sec.$^{-1}$	3,05.10^{-4}
	440	68,1	1,26
	300	100	0,71
D (énolique)	465	64,5	2,4
	265	113,0	0,96
AgD	480	62,5	1,18
CuD_2	555	54,0	2,84
	310	96,7	1,52
CuD	455	65,9	0,92
	308	97,3	0,50
HgD_2	483	62,0	5,32
	310	96,7	1,66
HgD	500	60,0	0,95
	300	100,0	1,00
ZnD_2	635	47,2	1,52
	520	57,6	5,76
	280	107,0	2,10
CdD_2	540	55,5	12,20
	285	105,5	2,52
PbD_2	522	57,5	5,64
BiD_3	490	61,2	7,17

Spectres d'absorption. (*A*) *Dithizone.* Le dithizone de la forme cétonique dissous dans le tétrachlorure de carbone donne trois bandes d'absorption dont les longueurs d'onde sont respectivement chaque pouvoir absorbant maximum aux 620 mμ, 440 mμ et 300 mμ. Nous les appelons la première, deuxième et troisième bande d'absorption d'après la longueur d'onde. La forme énolique du dithizone peut être obtenue en aioutant 0,2 normal d'ammoniaque au même volume de sa solution du tétrachlorure de carbone et en remuant ces mélanges. Le dithizone se transmet complètement à la couche aqueuse par ce traitement et se change en forme énolique. Dans ce cas, pour mesurer l'aborption lumineuse, on met 0,2 normal d'ammoniaque dans le contenant du dissolvant pour compenser l'absorption du dissolvant. La forme énolique donne une bande claire à 465 mμ dans la région visible, et une bande vague à 265 mμ environ dans la région ultraviolette.

(*B*) *Complexes métalliques du dithizone.* Suivant H. Fischer[2] nous avons préparé les solutions de certains complexes dissous dans le tétrachlorure de carbone par les réactions entre le dithizone en solution du tétrachlorure de carbone et des sels métalliques en solution aqueuse.

(1) AgD: Ce sel peut être obtenue comme la forme cétonique de sa solution acidique. Sa solution du tétrachlorure de carbone est jaune, et montre une bande d'absorption à 480 mμ, perdant la première et la deuxième bande de la forme cétonique du dithizone. Son absorption est semblable à celle donnée par la forme cétonique du dithizone lui-même dans la régien ultraviolette, mais nous ne sommes pas capables de mesurer la longueur d'onde du côté plus court, parce qu'elle est couverte par l'absorption du tétrachlorure de carbone lui-même.

(2) CuD_2: La solution du tétrachlorure de carbone de la forme cétonique a été préparé de la solution acidique du sel cuivrique en montrant la couleur violette et une bande à 555 mμ. Elle présente encore une bande distincte à 310 mμ qui est corréspondante à la troisième bande da la forme cétonique du dithizone.

(3) CuD: La forme énolique obtenue de la solution aqueuse neutre du sel cuivrique et la solution du tétrachlorure de carbone est brune. Cette solution présente deux bandes d'absorption à 455 mμ et 308 mμ. La première est plus hypsochromique que celle de CuD_2. La raison de ce phénomène nous semble être dans la constitution du radical thiocarbonyle $S = C<$ qui devrait peut-être changer en $-S-C\lessdot$.

(4) HgD_2: La solution acidique du sel mercurique où se trouve comme la forme cétonique est jaune-orange, et montre une bande à 483 mμ dans la région visible et une autre à 310 mμ environ dans la région ultraviolette.

(5) HgD: C'est la forme énolique préparée de la solution neutre qui donne la couleur rouge et le pouvoir absorbant maximum à 500 mμ.

La position de cette bande est influencée et plus bathochromique que celle de HgD_2, mais l'absorption ultraviolette est semblable à celle de HgD_2.

(6) ZnD_2: La forme cétonique peut être obtenue de la solution acidique. La couleur de cette solution est rouge-violette et donne deux bandes dans la région visible qui présetent respectivement leur maxima à 635 mμ et 520 mμ. La première bande coïncide à la position de celle de la forme cétonique du dithizone. On ne peut pas exactement juger si ce résultat est dû à l'absorption du dithizone lui-même donnée par la décomposition du complexe ou dû à une nouvelle absorption spécialement produite.

(7) CdD_2: La solution faiblement alcalisée de ce composé donne sa forme cétonique. Cette solution est rouge et montre une bande ayant le pouvoir fortement absorbant. Cette bande se trouve à 540 mμ, mais elle n'est pas distincte comme celle présentée par ZnD_2.

(8) PbD_2: La solution rouge de la forme cétonique montre une bande à 552 mμ. On ne pouvait trouver nulle absorption maximum jusqu'à 270 mμ dans la région ultraviolette, et c'est encore difficile de la mesurer dans cette région par la bande d'absorption du dissolvant tetrachlorure de carbone.

(9) BiD_3: La forme cétonique orange qui possède trois molécules du dithizone peut être obtenue de la solution neutre. Cette solution donne une bande large à 490 mμ dans la région visible. On ne peut cependant trouver l'absorption maximum dans le domaine ultraviolet comme dans le cas de PbD_2.

Résumé.

(1) Nous avons mesuré les absorptions lumineuses en région visible et ultraviolette du dithizone et ses complexes métalliques (Ag, Cu, Hg, Zn, Cd, Pb et Bi) dans leurs solutions du tétrachlorure de carbone.

(2) Les bandes d'adsorption be ces complexes métalliques donnent généralement deux bandes en région visible et ultraviolette. La première en région visible change sa position du pouvoir absorbant maximum suivant la sorte de métaux combinés, mais la longueur d'onde d'absorption du pouvoir maximum de la deuxième bande est à peu près invariable et grossièrement coïncide à celle du dithizone, lors même que les métaux combinés changent.

Laboratoire de Chimie minérale, Faculté des Arts et Métiers de Tokyo
(Tokyo Kogyô-Daigaku)

Actinomycin J_2, a By-product from a Strain of Actinomyces.

By Yoshimasa HIRATA and Koji NAKANISHI.

(Received January 22, 1949.)

An antibiotic (activity: 1:10,000,000 against *staphylococcus aureus Terajima*) has been obtained from *actinomyces flavus*,[1] which seems to be related to actinomycin A of Waksman[2], but considering the fact that the position of the absorption maximum in 95 % alcohol is 435 mμ, compared with the values 450 mμ and 230~250 mμ obtained by Waksman. and that there is a difference in the percentage of carbon (author: 55. 45 %, Waksman: 59.01 %), it is suggested that this substance is not quite identical which actinomycin A. Thus we shall call this substance actinomycin J_1. Meanwhile, another antibiotic, with a minor activity (1:160,000) seemed to have been extracted from the same strain, corresponding to actinomycin B of Waksman. We have studied its chemical structure and finally come to the conclusion of its being the dodecyl ester of 5-ketostearic acid:

$$CH_3(CH_2)_{10}CH_2OCO(CH_2)_3CO(CH_2)_{12}CH_3$$

by means of synthesis. Though this synthesized sample was identical with the natural specimen, it demonstrated no activity. Therefore, it must be concluded that the activity must have been due to a minute amount of the former actinomycin J_1 existing as an impurity in the second substance.

This second substance may be named actinomycin J_2 for convenience, notwithstanding its inactivity, and the experimental data for the determination of its chemical structure and synthesis are here reported.

Actinomyces flavus was cultivated on a Czapeck-Dox solution, extracted after two weeks and crystallized from methanol (m. p. 59–61° C).

It possesses a waxlike nature and odor, dissolving in all the wax-dissolving solvents. The fact that the ultra-violet absorption spectra showed no selective absorption suggested that it was probably a simple aliphatic compound containing none of the specific groups. The tetranitromethane and bromine tests were negative, thus excluding the presence of a double bond. Analysis gave the formula $C_{30}H_{58}O_3$(I), and by the action of ethanolic potassium hydroxide, the original substance was hydrolysed into two fractions, $C_{12}H_{26}O$ (II) and $C_{18}A_{36}O_3$ (III). (Scheme I)

(1) Y. Hirata and K. Nakanishi, *J. Penicillin*, 2 (1949), 180.

(2) S. A. Waksman and H. B. Woodruff, *J. Bact.*, 40 (1940), 583; *J. Biol. Chem.*, 142 (1942), 519.

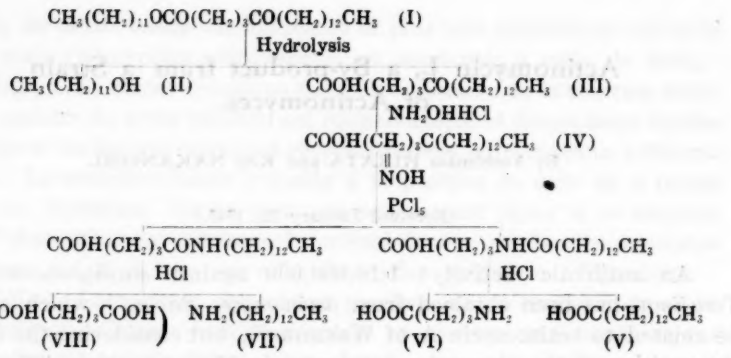

Bubbles which were generated by the action of sodium bicarbonate showed (III) to be an acid, while the negative results obtained from an effort to esterify the substance by means of *p*-nitrobenzoyl chloride and to dehydroxylize it by reduction with hydroiodic acid in a sealed tube, indicated that (III) was not a hydroxy acid. On the other hand, such derivatives as the 2,4-dinitrophenyl hydrazone and the oxime (IV) showed it to be a keto acid. The oxime was submitted to the Beckmann rearrangement and after hydrolysis with hydrochloric acid, (V) (VI) and a minute amount of (VII) were obtained, thus suggesting its structure to be 5-keto-stearic acid. (VII) could not be identified.

The melting point of (II) (22°) and the *α*-naphthyl urethane (80°) corresponded with that of dodecyl alcohol. Therefore, the sturecture of J_2 was established to be the dodecyl ester of 5-keto-stearic acid and this was further proved by synthesizing the substance and mixing it with the natural specimen, upon which no depression of melting point was observed. The synthesis was carried out by two methods, of which the latter gave a considerable yield (42 %).

The first method, analogous to that employed by Robinson and Robinson[3] (scheme II) is concluded by gradual hydrolysis under three steps of Scheme II. First Method.

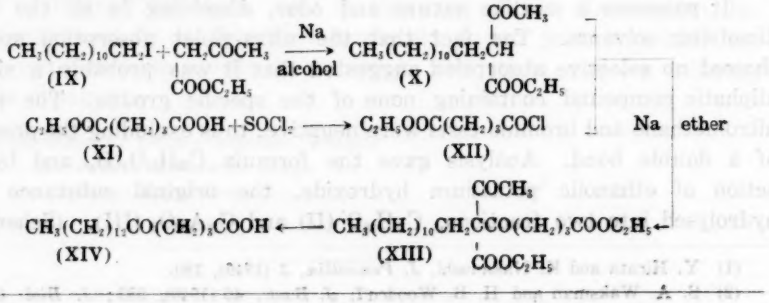

(3) G. M. Robinson and R. Robinson, *J. Chem. Soc.*, **127** (1925), 175.

Second Method.

$$\underset{\text{(XV)}}{Br(CH_2)_2COOC_2H_5} + \underset{\text{COOC}_2\text{H}_5}{\overset{\text{COCH}_3}{\overset{|}{\text{HCH}}}} \xrightarrow[\text{alc.}]{\text{Na}} \underset{\text{COOC}_2\text{H}_5}{\overset{\text{COCH}_3}{\overset{|}{\text{HC}}}}(CH_2)_2COOC_2H_5 + \underset{\text{(XVII)}}{CH_3(CH_2)_{12}COCl}$$

(XVI)

$$\xrightarrow[\text{ether}]{\text{Na}} CH_3(CH_2)_{12}CO\overset{\overset{\text{COCH}_3}{|}}{\underset{\underset{\text{COOC}_2\text{H}_5}{|}}{C}}(CH_2)_2COOC_2H_5 \longrightarrow \underset{\text{(XIX)}}{CH_3(CH_2)_{12}CO(CH_2)_2COOH}$$

(XVIII)

the condensation products of the form :

$$CH_3(CH_2)_m\overset{\overset{\text{COCH}_3}{|}}{\underset{\underset{\text{COOC}_2\text{H}_5}{|}}{C}}-CO(CH_2)_{12}COOC_2H_5$$

The process resulted in a very poor yield of the keto acid, owing to the fact that a considerable amount of the dibasic acid, $COOH(CH_2)_nCOOH$, and a ketone, $CH_3(CH_2)_{m+1}COCH_3$, were produced ; furthermore, it is rather tedious to prepare monoethyl glutarate (XI) in good yield. Bradley and Robinson[4] suggest that the hydrolysis of a series of substituted dibenzoyl methanes, $RCOCH_2COR'$ occurred with the production of the stronger of the acids, RCOOH and R'COOH in preponderating amounts. Thus in the diketo acids of the type shown above (XIII), owing to the fact that the dibasic acid, $COOH(CH_2)_nCOOH$ is stronger than acetic acid, the linkage marked with dots is degraded mainly, resulting in the undesired by-products, thd dibasic acid and a ketone.

In the second method (scheme II)[5] the synthesis was carried out by way of the diketo acid possessing the following general formula :

$$CH_3(CH_2)_{m+1}\overset{\overset{\text{COCH}_3}{|}}{\underset{\underset{\text{COOC}_2\text{H}_5}{|}}{C}}O(CH_2)_{n-1}COOC_2H_5$$

In this case, acetic acid is stronger than the acid, $CH_3(CH_2)_{m+1}COOH$, and this would make the hydrolysis proceed so as to give the desired keto acid, $CH_3(CH_2)_{m+1}CO(CH_2)_nCOOH$, as the main product.

Finally the synthesis of J_2, namely, the dodecyl ester of 5-ketostearic acid chloride was carried out by the reaction of dodecyl alcohol and the keto acid chloride in pyridine.

Experimental.

Cultivation. Actinomyces flavus (received from Dr. Umezawa)[6] was grown on a

(4) W. Bradley and R. Robinson, *J. Chem. Soc.*, **1926**, 2356.
(5) G. M. Robinson, *J. Chem. Soc.*, **1920**, 747.
(6) H. Umezawa, S. Hayano, T. Takeuchi and Y. Hara, *J. Penicillin.* **1** (1947), 123.

modified Czapeck-Dox medium ($NaNO_3$ 6 g., K_2HPO_4 2 g., KCl 1 g., $MgSO_4 7H_2O$ 1 g., $FeSO_4 7H_2O$ 0.02 g., glucose 60 g., peptone 10 g., distilled water 1000 c.c.) at 27°C for two weeks and shaken occasionally.

The culture liquid became brown-black and the floating bodies gradually acquired a yellowish color.

Extraction. The body and culture liquid were separated and the former extracted with acetone. The latter was shaken with clay and adsorbed, extracted with acetone, and the combined acetone solutions evaporated by submitting to a flash evaporator. The resulting orange yellowish turbid aqueous solution was extracted with ether, and red plates (actinomycin J_1) were obtained by concentrating the ether solution. After removing the crystals by decantation the concentration was repeated, upon which a second crop of J_1 precipitated. J_2 was obtained from the residue as white wax-like plates using methanol or ethanol as recrystallization solvent. Yields were 150 mg./l. and 80 mg./l. for J_1 and J_2 respectively. Melting point of J_2: 59-61°.

(Found: C, 76.36; H. 12.44. Calculated for $C_{36}H_{58}O_8$: C, 77.2; H, 12.5 %). Molecular weight determined by the Rast method gave 455. Calculated: 463.

Ultra-violet absorption spectra. The 0.1 %, 0.01 % and 0.001 % solutions in 96.5 % alcohol showed no selective absorption, the absorption of a 100 mm. solution beginning from 310 mμ.

Hydrolysis. Hydrolysis of J_2 was carried out by the action of 4 % alcoholic KOH on the sample (185 mg.) at room temperature for three days.

The alcohol was evaporated on a steam-bath and after addition of water to the residue, submitted to steam distillation, upon which (II) came over into the distillate as white crystals, possessing an odor of higher alcohol. The residue was acidified, extracted with ether, the ether evaporated and the residue (III) recrystallized from ethyl alcohol. m. p.: 81°. Found: C, 71.82; H, 13.05. Calculated for $C_{18}H_{36}O_3$: C, 72.0; H, 12.0%.

Dodecyl alcohol (II). M. p. 22°, alone or mixed with dodecyl alcohol. α-Naphthyl urethane: m. p. 79° (ligroin).

***p*-Bromophenacyl ester of 5-keto-stearic acid.** 1N NaOH was titrated to an alcoholic solution of the sample (25 mg.), using phenolphthalein as indicator. The solution should be kept slightly acidic and the concentration of alcohol kept above 70 %. One to two per cent. less than the equivalent amount of *p*-Bromophenacyl bromide is added to this solution, boiled on the bath under reflux for 1 hour, the flask cooled, water added and the separated solid recrystallized from dilute alcohol. m. p. 105° (uncorr.).

2,4-Dinitrophenyl hydrazone of 5-ketostearic acid. The alcohol and sulfuric acid solution of 2,4-dinitrophenyl hydrazine was added to the alcoholic solution of the keto acid and left overnight in the ice-box. After removing the red crystals of 2,4-dinitrophenyl hydrazine sulfate which may occur, the remaining red oil crystallized after 1-2 days. M. p. 110° (uncorr.).

5-Ketostearic acid oxime (IV). A mixture of the keto acid (70 mg.), anhydrous pyridine (1.3 c.c.) and hydroxyl amine hydrochloride (30 mg.) (molecular ratio; 1:1:3) was gently boiled for 3 hours under reflux, poured into water and acidified with HCl. The resulting oxime was extracted with ether, and crystallized from alcohol. This method using pyridine enabled the oxime to be prepared more easily and completely than the usual method with alcoholic KOH. m. p. 64°. Found: N, 4.90. Calculated for $C_{18}H_{37}O_2N$: N, 4.4 %.

Beckmann rearrangement and hydrolysis of the oxime (IV). PCl_5 was added under cooling with an ice-mixture to the dilute ether solution of the oxime obtained above and kept overnight ot 0°, A sufficient amount of PCl_5 should be added to retain a precipitate of PCl_5. The mixture is shaken with ice-water, the ether evaporated after drying over K_2CO_3 and the residue heated eight hours with conc. HCl at 160° in a sealed tube.

Myristic acid (V). Water is poured into the reaction mixture and the white crystals

extracted with ether. M. p. 53° (alcohol), alone or mixed with myristic acid. Found: C, 72.58; H, 12.01. Calculated for $C_{14}H_{28}O_2$: C, 73,7; H, 12.3 %.

***n*-Tridecyl amine (VII).** The acidic solution was made alkaline, extracted with ether and dry HCl gas passed through, upon which a small amount of fine white needles were obtained. Hygroscopic, decomposed at 100°. Pt-salt ($2C_{13}H_{29}N+2HCl+PtCl_4$): 230° (decomp.).

Glutaric acid (VIII). This was unobtainable owing to the minute amount of sample used.

γ-Aminobutyric acid (VI). The alkaline residue was acidified with HCl, evaporated on the water-bath, separated from NaCl by washing with absolute alcohol and the alcohol evaporated. The remaining syrup crystallized into hygroscopic needles when kept in an ice-box. The Pt-salt was obtained and analysed. Found: Pt, 31.02; Calculated for $2NH_2(CH_2)_3COOH+2HCl+PtCl_4$: Pt. 31.88 %.

Dodecyl-acetoacetic acid ethyl ester (X). Dodecyl iodide (IX) was prepared by passing HI gas (2.5 mol) through dodecanol (55 g., 0.3 mol) at room temperature, and after washing with water and dilute KOH, distilled; the portions 165-170°/20 mm. collected (40 g.).

16 g. of an oil, b. p. 205°/255 mm., were obtained according to the usual method, employing Na (2.1 g.), ethyl acetoacetate (17.7 g.), absolute alcohol (30 c c.), n-dodecyl iodide (28 g.): the time of reaction was 5 hours.

4-Carbethoxybutyryl chloride (XII). Monoethyl glutarate (XI) was prepared by a method analogous to that employed by Grün and Wirth[7] in the semihydrolysis of diethyl sebacate; namely, diethyl glutarate (8 g.) was dissolved in half its volume of absolute alcohol and to this boiling solution a calculated amount of 2 N KOH alcoholic solution was added under vigorous stirring. The resulting white mass was poured into a considerable amount of ice-water, and the alcohol removed by distillation under reduced pressure. After extracting the unchanged diester completely with ether, the residue was acidified and extracted with ether. A crude product of the monoester was obtained by evaporating the ether. The ether extract was dried over Na_2SO_4 and distilled. 3 g. of an oil, 143°/7 mm. was obtained. Monoethyl glutarate (1.8 g.) was heated gently on the water bath with thionyl chloride (6 g.) for 3 hours, the excess thionyl chloride removed completely by distillation under reduced pressure and by keeping the residue in vacuum. A high temperature should be avoided throughout all the processes, owing to the unstability of the monoester, The chloride (XII) thus obtained was directly submitted to further procedures.

5-Ketostearic acid (XVI) (First method). Na (0.28 g.) was granulated under toluene, washed with ether, suspended in ether (20 c.c.) and (X) gradually added, the clear solution of the sodio derivative being completed by heating on the bath for several minutes. To this solution, 4-carbethoxy-butyryl chloride (XIII) dissolved in ether (3 c.c.) was added at 0°; after remaining 30 minutes at room temperature, the mixture was boiled under reflux for 15 minutes, cooled, washed with water and the ether evaporated. The residue was agitated for 8 hours with 5 % NaOH (75 c.c.), acidified with acetic acid and collected by means of ether. The product was next boiled with 5 % H_2SO_4 (100 c c.) for 8 hours and steam-distilled in order to remove the methyl tridecyl ketone. The hydrolysis was completed by boiling with 5 % NaOH (400 c.c.) for 5 hours. The product crystallized from light petroleum ether (b. p. 40-80°) and methyl alcohol, but the yield was poor, m. p. 81.5°, alone or mixed with the natural keto acid.

Diethyl α-acetoglutarate (XVI). Ethyl 3-bromopropionate (XV) (11.4 g.) ("Organic

(7) A Grün and T. Wirth, *Ber.*, 55 (1922), 2207.

Synthesis" Coll. Vol. I, p. 263) Na (2.6 g.), absolute alcohol (57 c.c.) and ethylacetoacetate (14.8 g.) were submitted to the usual method, the time of reaction being 5 hours. 2.8 g. of an oil, 158-162°/15 mm. were obtained.

5-Ketostearic acid (Second method) (XIX). Na (0.3 g.) was granulated under toluene, washed with ether, suspended in ether (30 c.c.), and diethyl α-acetoglutarate (XVI) (2.8 g.) gradually added (30 minutes) upon which the sodio-derivative was produced as a white powder. After the addition of myristic acid chloride (XVII) (3 g.), the mixture was left overnight to complete the precipitation of NaCl, boiled under reflux for 20 minutes, washed with water, the ethere evaporated and the residue agitated with 3% NaCH (170 c.c.) for 9 hours. The solution was concentrated for one hour on the bath, upon which the crude Na-salt of the keto acid formed a gelatinous mass. The free acid, prepared by the treatment with HCl and extraction with ether, was crystallized from light petroleum ether (b. p. 40-80°) and methyl alcohol. M. p. 81°, alone or mixed with the natural specimen. Yield: 1.5 g. or 42%.

Actinomycin J_2. 5-Ketostearic acid (350 mg.) was converted into its chloride by the action of thionyl chloride at 50°, the excess reagent being removed by reduced pressure. A solution of dodecyl alcohol (250 mg.) in pyridine (3 c.c.) was added to the chloride, heated at 50° for 5 minutes, left overnight at room temperature, poured into water and extracted with ether. The ethereal solution was washed with dil. H_2SO_4 and water, the ether evaporated and the residue dissolved in hot alcohol. The plates which appeared on cooling seemed to be a mixture of dodecyl alcohol and the keto acid. After removing this portion, the ester was obtained by concentrating the remaining alcoholic solution. M. p. 60°, alone or mixed with the natural substance.

Summary.

The constitution of actiomycin J_2 obtained from *actinomyces flavus* has been studied and idenified to be the dodecyl ester of 5-ketostearic acid by means of hydrolysis of the original substance, followed by the Beckmann rearrangement and hydrolysis of the oxime of 5-ketostearic acid into myristic acid, γ-aminobutyric acid and a small amount of *n*-tridecyl-amine. Next, the 5-ketostearic acid was synthesized according to two methods, which were concluded respectively by the hydrolysis of condensation products of the type: $CH_3(CH_2)_mC(COCH_3)(COOC_2H_5)CO(CH_2)_nCOOC_2H_5$ and $CH_3(CH_2)_{n+1}CO(COCH_3)(COOC_2H_5)(CH_2)_{n-1}COOC_2H_5$, of which the latter gave a considerable yield, while that of the former was very poor owing to the undesired direction of hydrolysis. The condensarion products of 5-ketostearic acid chloride and dodecyl alcohol showed no depression of meltihg point when mixed with actinomycin J_2, thus proving the constitution of actinomycin J_2 to be the dodecyl ester of 5-ketostearic acid.

These experiments were begun since it seemed that actinomycin J_2 was an antibiotic, but considering the fact that the synthesized specimen demonstrated no such activity, it must be conculded that the original activity was probably due to a minute amount of actinomycin J_1 existing as an impurity, and that actinomycin J_2 is a mere by-product.

In conclusion, the authors wish to acknowledge their indebtedness to

Profs., F. Egami, K. Yamazaki, W. Kimura, H. Umezawa and Ass. Prof. H. Kubo for their kind encouragements and valuable advices given in the course of this study.

Chem. Institute, Faculty of Science.
Nagoya University.

On the Catalytic Decomposition of Carbon Monoxide by Iron.

By **Hideo AKAMATU** and **Kazutoshi SATÔ.**

(Received January 30, 1949.)

Introduction. It is known that carbon monoxide is decomposed catalytically by iron or the other transition metals, and free carbon is formed. Studies on this phenomenon were carried out on the standpoint of chemical kinetics by some investigators[1]. It was also pointed out by U. Hofmann[2] and T. Watanabe[3] that the free carbon formed by the decompcsition of carbon monoxide on iron surface has graphitelike properties. Commonly, carbons are amorphous, as soot or carbon black, when they are formed by thermal decomposition of carbon compounds. In order to graphitize them, it is necessary to heat them again over the temperature of 2500°C at least. If carbon which is formed by the catalytic decomdosition of carbon monoxide at comparatively low temperature such as 500°C, is already graphitized, there must be some special reason for this graphitization.

To find the mechanism of this reaction, we investigated the changes of the structure of iron surface (catalyser) at some intermediate stages of the reaction by the method of electron diffraction.

Experimental and Results. The experimental procedure was not much different from those which had been used by former investigators. Carbon monoxide, produced by the reaction with formic acid and concentrated

(1) H. A. Bahr, *Ber.*, **61** (1928), 2177; **63** (1930), 2226; H. A. Bahr and V. Jessen, *Ber.*, **66** (1933), 1238; U. Hofmann, *Ber.*, **61** (1928, 1180; U. Hofmann and E. Groll, *Z anorg. allgem. Chem.*, **191** (1930), 414; U. Hofmann and D. W. Münster, *Z. Elektrochem.*, **42** (1936), 504; H. Tsuchiya, *Bull. Inst. Phys. Chem. Research (Tokyo)*, **8** (1929), 206, 609; **10** (1931), 556, 951; S. Horiba and Taikei Ri, *Rev. Phys. Chem. (Japan)*, **2** (1928), 11; **4** (1930), 73; **5** (1931), 41; F. Olmer, *J. Phys. Chem.*, **46** (1942), 405.

(2) U. Hofmann, *Ber.*, **61** (1928), 1180.

(3) T. Watanabe, *Bull. Inst. Phys. Chem. Research (Tokyo)*, **7** (1928), 1077; **8** (1929), 288.

sulphuric acid, was flowed into the reaction tube from the reservoir after passing through a dryer such as concentrated sulphuric acid and phosphoric anhydride. For the reason which will be described in the latter section, attention was paid to remove the trace of oxygen in the reaction gas. For this purpose, the gas was passed through the basic solution of potassium pyrogallate and then the heated copper gauze.

The reaction tube was a quartz tube, a part of which could be heated by an electric furnace. The furnace was a small type one, of which length was about 20 cm., and could be slid along the reaction tube. To take out the catalyser from the reaction tube at a certain stage of the reaction, the electric furnace was slid off and the tube could be quickly cooled.

A piece of iron, Kahlbaum's electrolytic iron, was used as catalyser. For the investigation by the electron diffraction method, the surface of the catalyser was polished to flatness by emery paper. To set the catalyser in the reaction tube, a porcelain boat was used.

The gas flowing out from the reaction tube was exhausted after passing through the baryta solution. This solution will be turbid with carbon dioxide when the reaction proceeds as $2CO \rightarrow C + CO_2$.

It took commonly 5~10 hours till the decompositian began to proceed, under the condition in which the reaction temperature was 500°C, and the flowing velocity of carbon monoxide was 400 c.c. per hour. Once the reaction began to proceed, however, the decomposition took place smoothly and free carbon would be formed gradually on the surface of the catalyser.

The electron diffraction patterns of the surface of the catalyser were taken at two intermediate stages of the reaction. The first was when the decomposition had just begun to proceed, that was after a short time when the turbidness of the baryta solution by CO_2 had begun to take place. At this stage, free carbon was not yet found on the catalyser, while the iron surface had lost metallic lustre and become opaque. The observed values of the electron diffraction pattern are shown in Table 1. It is quite different from the pattern of pure iron. It was proved that this pattern belongs to that of cementite. In Table 1, the x-ray diffraction data of cementite[4] are also shown. Both spacings observed by x-ray and electron diffraction coincide satisfactorily with each other. From this result, it was found that at the first stage of the reaction cementite had been formed on the surface of iron catalyser.

The second electron diffraction pattern was taken when further decomposition had proceeded (after 15 hours from the beginning). At this stage, the surface of the catalyser was changed to black or blacky

(4) The X-ray data of cementite are taken from the values observed by A. Ōsawa and S. Takeda, *Kinzoku no Kenkyu*, **8** (1931), 181.

Table 1.

The electron diffraction pattern of the surface of the ironcatalyser at the first stage of the reaction. (Cementite).

Values of Spacings observed by Electron Diffraction		Corresponding x-ray Data for Cementite.		
2.10 Å	w.	2.10 Å	m.	(210)
2.025	m.	2.01	v.s.	(211), (103)
1.86	m.	1.855	v.s.	(122), (113)
1.685	w.	1.675	m.	(023)
1.59	w.	1.58	m.	(123), (014)
1.51	w.	1.50	m.	(301)
1.36	v.w.	1.36	m.	(302), (320)
1.21	v.w.	1.21	v.s.	(141)
1.155	w.	1.155	v.s.	(142), (403),
1.125	m. diffuse.	1.121	v.v.s.	(240)
0.912	w.			
0.795	m.			

grey clolor in parts, but carbon had not yet been separated in powder form. The spacings observed from this pattern are shown in Table 2. It consists of the carbon pattern principally, but some spacings belonging to cementite are also found. The latter were weak. By using the shorter wave of the cathod-ray, however, the reflected rings belonging to cementite could be made strong to a certain degree. It was known from this fact that the ground substance was also cementite underlying the carbon layer.

Table 2.

The electron diffraction pattern of the surface of the catalyser at the second stage of the reaction.

Values of Spacings observed by Electron Diffraction		Corresponding Indices of Graphite		or	Cementite.			
3.40 Å.	v.s.	(002)	3.39 Å.					
2.12	s.	(100)	2.12					
2.03	m.	(101)	2.02					
1.85	w.				(122),	(113)	1.855	Å
1.69	m.	(004)	1.69					
1.228	s.	(110)	1.228					
1.17	m. diffuse.	(112)	1.150					
1.125	m. diffuse.	(006)	1.120		(240)		1.121	
1.056	w.	(201)	1.049		(225)		1.050	
0.981	w.	(106)	0.991		(413)	(422) (340)	0.99	

When the decomposition proceeded further, the surface of the cata-

lyser was covered all over by a carbon layer which took the powder form. The electron diffraction pattern was also attributed to carbon alone, and the cementite pattern could not be found already because of the existence of a thick layer of carbon.

On the Structure of Carbon produced by this Reaction. It has been pointed out that the crystal structure of so-called amorphous carbon is somewhat different from that of graphite[5]. In graphite, the three-dimensional atomic lattice is completed by a definite arrangement of atoms along every crystal axis. On the other hand, in amorphous carbon, the complete three-dimensional atomic lattice is not produced. It is made of pseudo-crystals, or it would be better to say, a kind of layer lattice consisting of hexagon planes of carbon atoms. The hexagon planes of carbon atoms are arranged in such a way that although they are parallel to each other along the *c*-axis, still along the *a*- or *b*-axis they are not arranged in any definite manner. For this reason, x-ray or electron diffraction patterns from amorphous carbons lack the spacings corresponding to the general indices (*hkl*) excepting (*hk*0) and (00*l*). As well known, the pattern of amorphou scarbon consists of small numbers of diffused rings corresponding to (002), (100) and (110), and lacks other spacings such as (101) and (112) which are comparatively strong rings in the case of graphite. Thus, it may prove to be graphite, when the spacings corresponding to (101) and (112) be found in the pattern of carbon.

The observed pattern, as shown in Table 2, consists of many sharp rings. They can correspond to carbon and cementite respectively. There are also same spacings which can not be made distinct whether they are attributed to carbon or cementite, for the same values may be found in both substances. However, the spacings corresponding to the values of 2.03 Å can be attributed to graphite at least, for they are moderately strong in comparison with the ring of 1.85 Å, this latter being the typical ring of cementite. From this fact and the sharpness of reflected rings, the whole appearance of the pattern closely resembles the graphite pattern. It will be possible to conclude reasonably that the carbon formed at the early stage of the decompositjon is not amorphous but is graphitized.

On the Poisoning Action by Oxygen. It has been known already that in this reaction the catalyser is poisoned by some substances such as sulphur or arsenic compounds[3]. We found that the reaction is also hindered by the existence of oxygen. When the pulverized iron was used as catalyser, the poisoning effect by the trace of oxygen was not so

(5) H. Akamatu. *J. Chem. Soc. Japan*, **64** (1943), 1251; H. Akamatu and K. Nagamatsu, *J. Colloid Science*, **2** (1947), 593.

remarkable as to be noticed. However, when an iron plate was used as catalyser, the decomposition did not proceeded when a trace of oxygen existed in the carbon monoxide. In the latter case, we found that the oxide layer had been formed on the surface of the catalyser. By the electron diffraction, it was proved that the layer was made of Fe_3O_4 or sometimes of Fe_2O_3.

Summary and Conclusion. It was found that carbon produced by catalytic decomposition of carbon monoxide by iron is not amorphous carbon as ordinary soot, but seems to be graphite, at least at the early stage of the decomposition. It was found by the electron diffraction that at the first stage of this reaction, cementite is formed on the surface of iron. It was also found that the catalytic decomposition of carbon monoxide never takes place if iron is oxidized before cementite is formed.

From these results, it will be concluded that carbon is produced by the decomposition of cementite, in other words, cementite is one of the intermediate compounds, at least, which is formed before free carbon is separated. This conclusion suggests that the reaction takes place following the schema as:

$$3Fe+2CO \rightarrow Fe_3C+CO_2$$
$$\hookrightarrow 3Fe+C.$$

This conclusion is not far from that assumed by some of the former investigators. Some investigators have assumed that Fe_2C also is the other intermediate compound, but we have not yet found it by our experiments carried out at 500°C.

It is interesting also that carbon has the structure of graphite when it is separated from cementite.

In conclusion, the authors wish to express their thanks to Prof. J. Sameshima for his kind encouragement through the experiment. A part of the cost of this study was defrayed from the grant of the Ministry of Education, to which thanks are due.

Chemical Institute, Faculty of Science,
Tokyo University, Tokyo.

A Stereochemical Representation of the Structures and the Scission Reactions of Cholesterol Oxides.[1]

By Yoshiyuki URUSHIBARA.

(Received February 7, 1949.)

In a previous paper[2] the results of the studies on the scission reactions of the oxido ring in cholesterol oxides by the author and M. Chuman were briefly described. They include (i) reduction with sodium and amyl alcohol, (ii) catalytic reduction, (iii) action of aluminium amalgam and of aluminium isopropylate and isopropyl alcohol, (iv) hydration, and (v) action of Grignard's reagent. Besides those already cited there, the reactions of cholesterol oxides or their esters with hydrogen chloride,[3] with acetic acid,[4][5] and with methanol in the presence of sulfuric acid,[4] have been investigated by other authors. The results hitherto gathered may be summarized as follows:

The oxido ring in α-cholesterol oxide (I) or its esters is opened always but one exception between carbon atom 6 and the oxido oxygen atom, and the oxygen atom with the hydrogen atom derived directly or indirectly from the addenda forms a hydroxyl group attached to carbon atom 5 with the original α-configuration, while the residues from the addenda become attached to carbon atom 6, the configuration being determined to be β for certain residues, perhaps undetermined for the chlorine atom, assumed α for the methyl group from Grignard's reagent, and meaningless for the hydrogen atom from reduction (I→III). An exception is encountered in the reduction with sodium and amyl alcohol, where the oxido ring is opened between carbon atom 5 and the oxygen atom, and the carbon atom 5 maintains the original α-configuration producing a cholestane derivative.

As for β-cholesterol oxide earlier works were carried out with impure specimens or the molecular compound with the α-isomeride, and the results obtained must be considered with reserve. Experiments with pure specimens have shown that the oxido ring in the β-oxide or its esters is opened, without exception, between carbon atom 5 and the oxido oxygen atom. The oxygen atom takes the hydrogen atom coming directly or

(1) An abridged account was read before the 68th annual meeting of the Chemical Society of Japan on October 18th, 1946.

(2) Y. Urushibara and M. Chuman, this Bulletin, 22 (1949), 69.

(3) F. S. Spring and G. Swain, *J. Chem. Soc.*, 1939, 1356; L. Ruzicka and W. Bosshard, *Helv. Chim. Acta*, 20 (1937), 244.

(4) J. Hattori, *J. Pharm. Soc. Japan*, 59 (1939), 411; 60 (1940), 334.

(5) M. Ehrenstein, *J. Org. Chem.*, 6 (1941), 626.

indirectly from the addenda and forms a hydroxyl group attached to carbon atom 6 with the original β-configuration, while carbon atom 5 cut off from the oxygen atom gains the residues from the addenda, and the configuration around this asymmetric centre is always α, as far as determined, giving rise to the formation of cholestane derivatives but never of coprostane derivatives which might be expected (II→IV).

Ruzicka and co-workers[6] constructed models for saturated and unsaturated sterols, where they related free or hindered rotation of the hydroxyl group at carbon atom 3 about the oxygen-carbon bond to the velocity of saponification of esters and took into account the flat molecular structures of the steroids demonstrated by Bernal. Thus, the free hydroxyl group of the cholestanol model and the hindered one in the coprostanol model were made to correspond respectively to the greater and the smaller velocities of the saponification of the esters. In the accompanying formulas, (V), (VI), and (VII), borrowed from their figures, substituents directed to the same side of (over, as generally formulated) the plane of the ring system are indicated by thick dots and letter S shows the cyclohexane ring concerned being in a chair form. If it is desired to visualize the actual models better than by these formulas, the pictures in the original paper may advisably be consulted.

Although the formulas, and even the pictures of the models, hardly permit to perceive it at a glance, ring A has a chair form in the same manner of zigzag in cholestanol and in cholesterol, while in coprostanol the zigzag is in an inverse manner. In other words, if in the cholestanol and cholesterol models carbon atoms 1, 3, and 5 are situated downwards or at the bottoms of the zigzag, in the coprostanol model carbon atoms designated by the same numbers are placed upwards or at the tops of the zigzag. Moreover, in the cholestanol and cholesterol models an axis passes straight through the whole ring system, while the coprostanol model, owing to the cis linking of rings A and B, is remarkably folded at this linking.

An introduction of a double bond between carbon atoms 5 and 6 is possible only with ring A of cholestanol, and impossible with ring A of coprostanol, because the ethylene system will tend to be coplanar. On the other hand, a double bond can enter between carbon atoms 4 and 5 of ring A of either cholestanol or coprostanol; or, more precisely, the coplanar ethylene system comprising five carbon atoms 3, 4, 5, 6, and 10 and one hydrogen atom at 4 with a double bond between 4 and 5 is compatible with carbon atoms 1 and 2 as they are either in cholestanol or in coprostanol. The above consideration may be useful for reminding that Δ^5-steroids are generally

(6) L. Ruzicka, M. Furter, and M. W. Goldberg, *Helv. Chim. Acta*, 21 (1938), 498.

hydrogenated to cholestane derivatives[7] and Δ^4-steroids to either cholestane or coprostane compounds.

Now, the influence of a 5,6-oxido ring upon the form of ring A will be considered. The three-membered ring is equivalent or similar to

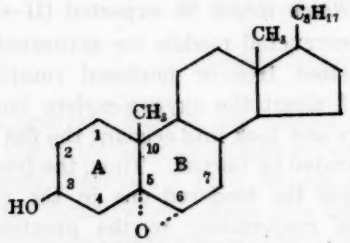

(I) α-Cholesterol oxide

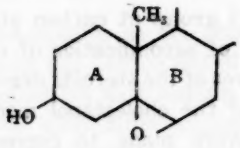

(II) β-Cholesterol oxide

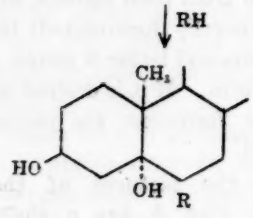

(III)

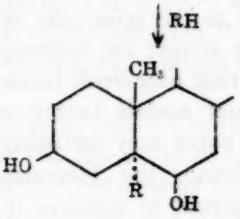

(IV)

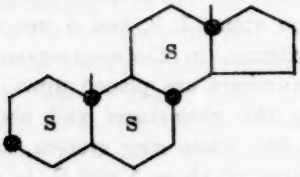

(V) Cholestanol

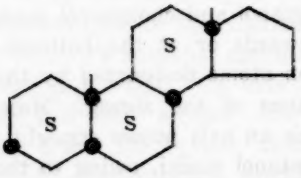

(VI) Coprostanol

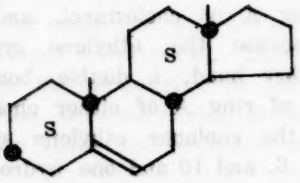

(VII) Cholesterol

(7) Cholestene gives two stereoisomeric hydrochlorides, J. Mauthner, *Monatsh.*, **28** (1907), 1113; T. Kon, *J. Pharm. Soc. Japan*, **65** (1945), 63, but is an explanation not plausible that pseudo-cholestene (coprostene) may intervene in the reaction?

the double bond in causing a structural restriction. The elements of symmetry found in the ethylene system still survive the destruction of the coplanarity by the three-membered ring introduced perpendicularly to the ethylene plane. Here, symmetry refers of course only to the arrangement or direction of the four atoms, other than the oxido oxygen atom, directly attached to carbon atoms 5 and 6, the nature of the four groups and the bond lengths being ignored. Thus, planes of symmetry in this sense exist within the segment of the molecule concerned, one passing through the three-membered ring and another through the oxygen atom and perpendicular to the former and to the bond between carbon atoms 5 and 6. The tendency of carbon atoms 10, 4, and 7 and the hydrogen atom at 6 to be arranged or directed symmetrically with reference to these planes excludes again ring A of coprostanol, irrespective as to whether the three-membered ring is α-oxidic or β-oxidic.

In this respect, not only α- but also β-cholesterol oxides must be considered as a derivative of cholestanol. When the β-oxide was called 5,6-epoxy-coprostanol-(3β)[8] by a term representing the structure, it was presumed automatically to be a coprostane derivative from the β-configuration of the linkage between carbon atom 5 and the oxygen atom; but in conformity with the real aspects of the spatial constitutions the β-oxide must be called 5,6β-epoxy (or oxido)-cholestanol-(3β), and 5,6α-epoxy (or oxido)-cholestanol-(3β). for the α-oxide cannot dispense with Greek letter α.

Before entering the next step of the stereochemical representation, the characteristics of the cleavage reactions of the oxido ring which are to be explained thereby will be summarized again in a shorter expression: The oxido ring in the α-oxide is ordinarily opened between carbon atom 6 and the oxygen atom, but can be split at the other linkage. Cleavage occurs always between carbon atom 5 and the oxygen atom in the β-oxide. The most important point is that cholestane derivatives, but none of coprostane derivatives, are produced in all the scission reactions of not only α- but also β-cholesterol oxide. Now, the stereochemical investigation affords a reasonable explanation of such behaviours of the oxides. Ring A in both α- and β-cholesterol oxides being of the same cholestanol type, the formation of cholestanol derivatives from both must be exclusive, as cholestanol is formed preferentially by the hydrogenation of cholesterol, unless a ring conversion takes place; and the formation of cholestanol derivatives from the α-oxide is possible for either of the alternative cleavage points, but that from the β-oxide is possible only when the oxido ring is opened between carbon atom 5 and the oxygen atom and thus when carbon atom 5 is given temporarily a free valency in order to be capable of adapting itself to ring A.

(8) Y. Urushibara, this Bulletin, 16 (1941), 182.

Suppose the oxido ring in the β-oxide were split between carbon atom 6 and the oxygen atom, then ring A of the cholestanol type and carbon atom 5 holding the oxygen atom in the β-configuration would be incompatible and must be reconciled only at the expense of an excessive work of either changing the former into the coprostanol type or inverting the latter to the α-configuration. While there may be no question as to stating that an inversion at carbon atom 5 would be difficult, or even impossible, so long as the oxygen atom remained attached there, the possibility of the conversion of ring A may be examined more closely. The conversion of ring A from the cholestanol type to the coprostanol type has been attained from Δ^5-steroids through the versatile Δ^4-ring, while the reverse ring conversion has been experienced, necessarily associated with the rearrangement of the configuration at carbon atom 5 from β to α, when a hydrogen atom is present at carbon atom 5 and at the same time a carbonyl group exists at an adjacent carbon atom, perhaps through an enolization and thus through a Δ^4- or Δ^5-intermediate. Such an interconversion of ring A involving a participation of an unsaturated intermediate could not be effected in a compound with an oxygen atom attached to carbon atom 5. A direct transformation of the cholestanol type into the coprostanol type might be possible, inasmuch as an oxygen atom bound to carbon atom 5 in the β-configuration were found favoring it, but it would not be so easy as expected from a mere consideration of the lability of a simpler cyclohexane ring, owing to the more profound difference between the cholestanol and the coprostanol rings and the structural restriction imposed by the surroundings. Thus, if the cleavage should occur between carbon atom 6 and the oxygen atom, then the process would be completed by giving a coprostanol derivative resulting from the conversion of ring A rather than a cholestanol derivative requiring the inversion at carbon atom 5; but even the trouble involved in this ring conversion appears to be enough for preventing such a fission from taking place and for giving way to the other fission that can be settled more smoothly. In other words, the linkage will resist such a fission as would be associated with more later work. It may be again emphasized in this connection that a transformation of ring A does not take place even in the hydrogenation of Δ^5-steroids. The hydroxyl group or its equivalent at carbon atom 3 may add the difficulty in the ring conversion, because the group freely rotatable in the cholestanol type must be confined in a sterically hindered position when the ring is converted into the coprostanol type, and it may be logically correct to mention that such a confinement itself will be confronted with a steric hindrance.

In the preceding paragraphs the structures of cholesterol oxides and the courses of scission reactions of the oxido ring in them have been elucidated on the basis of the spatial formulation elaborated by Ruzicka

and co-workers. If the stereochemical representation be feasible also in the cases of the oxides of other Δ^5-steroids, then the behaviours in scission reactions will give grounds for discussing the configuration of their oxido rings. Thus, in a separate paper it will be shown that the oxido rings in the oxides of Δ^5-cholestenone possess most probably the configurations contrary to the Greek letters arbitrarily prefixed in their names.

Chemical Institute, Faculty of Science,
Tokyo University.

Studies on Nitrate Reductase. III.[1][2]

By Ryo SATO and Fujio EGAMI.

(Received February 1, 1949.)

Introduction. Many species of bacteria are able to reduce nitrate to nitrite. The actual agency of this reduction, however, remained obscure until Quastel, Stephenson and Whetham[3] pointed out the existence of a specific enzyme acting on nitrate in Bac. coli and some other facultative anaerobes. In 1938–39 Yamagata[4] obtained a cell-free preparation of this enzyme and proposed the name "nitrate reductase" instead of "nitratase" which had been previously used. Recently we have succeeded in obtaining a cell-free preparation of nitrate reductase from Bac. coli by ultrasonic destruction of the cells and studied several properties and the mode of action of this enzyme.[1][2]

By these foregoing investigations it has been firmly established that nitrate reductase is an enzyme which catalyzes the oxidation of the reduced form of an intermediary hydrogen carrier by nitrate and therefore the biological reduction of nitrate consists of two steps even in the simplest case. This case may be shown schematically as follows:

$$\begin{array}{ccccc} \text{Hydrogen Donator} & \xrightarrow[\text{Dehydrogenase}]{} & \text{Intermediary Hydrogen Carrier} & \xrightarrow[\text{Nitrate Reductase}]{} & NO_3' \end{array} \qquad \text{(I)}$$

As the intermediary hydrogen carrier in this scheme, methylene blue or

(1) F. Egami and R. Sato, *J. Chem. Soc. Japan*, **68** (1947), 39.

(2) F. Egami and R. Sato, *J. Chem. Soc. Japan*, **69** (1948), 20; cf. F. Egami, *Chemical Researches*, **1** (1948), 117.

(3) J. H. Quastel, M. Stephenson and M. D. Whetham, *Biochem. J.*, **19** (1925), 304; cf. L. H. Stickland, *Biochem. J.*, **29** (1934), 1543; E. Aubel, *Enzymologia*, **4** (1937), 51, etc.

(4) S. Yamagata, *Acta Phytochimica*, **10** (1938), 283; **11** (1939), 145.

any other suitable oxidation-reduction indicator can be used *in vitro*. For the purpose of the study of nitrate reductase apart from dehydrogenase system, we have constructed the following system.

$$\text{Leucomethylene blue} \xrightarrow[\text{Nitrate Reductase}]{} NO_3' \qquad \text{(II)}$$

Here the leuco form of methylene blue is prepared chemically by catalytic hydrogenation of methylene blue using Pd-$BaSO_4$ as a catalyst.

Further we have shown that flavin-adenine-dinucleotide, and presumably also several flavoprotein enzymes, can act as intermediary hydrogen carriers. However we found an important exception to scheme (I) when succinate was supplied as a hydrogen donator. In this case the succinate-succinic dehydrogenase system can react directly with the nitrate-nitrate reductase system without auy intermediary hydrogen carrier.

$$\text{Succinate} \xrightarrow[\text{Succinic Dehydrogenase}]{} \xrightarrow[\text{Nitrate Reductase}]{} NO_3' \qquad \text{(III)}$$

It must be mentioned here that succinic dehydrogenase is known as a so-called "cytochrome reducing dehydrogenase".

All these findings provide an interesting information about the position of nitrate reductase in the reaction chains of biological oxidations. That is, nitrate reductase may perhaps play a similar rôle to that of the Warburg-Keilin system when nitrate is used as an ultimate hydrogen acceptor instead of molecular oxygen.

From these considerations we have been led to an assumption that the chemical nature of nitrate reductase might be similar to that of cytochrome or cytochrome oxidase. In the present paper studies on this line will be reported.

Experimental. Preparation of enzyme: Bac. coli was grown on peptone-bouillon-agar medium containing 0.1 % KNO_3 for 24 hours at 37°. Cells were harvested and washed several times with 0.8 % NaCl solution and suspended thickly in phosphate buffer (*p*H 7.4, $\frac{1}{10}$ mol). The suspension was then exposed to ultrasonic waves (500 KC., anode voltage 1200 volts) for 30 minutes and was centrifuged (10,000 r.p.m.) to remove cell debris completely. The supernatant fluid was dialysed overnight against streaming water. To this solution ammonium sulfate was added to an extent of 0.2 saturation and the precipitate was centrifuged off. Ammonium sulfase was again added to half saturation, and then centrifuged. The precipitate thus obtained was dried in a vacuum desiccator containing concentrated sulfuric acid. Thus we could obtain from ca. 50 g. wet cells ca. 1 g. of dried powder mixed with crystalls of ammonium sulfate.

This preparation can be kept for several months without inactivation in a desiccator at 0°. 300 mg. of this powder was dissolved in 10 c.c. of distilled water and used as a nitrate reductase solution. Besides nitrate reductase our preparation shows a powerful activity of formic dehydrogenase when tested with methylene blue technique. For the purpose of spectroscopic observations solutions containing 100 mg. of powder per c.c. were used.

Measurement of enzyme activity: Thunberg tubes were employed. Reaction mixture was usually as follows: 0.5 c.c. of enzyme solution, 1 c.c. of phosphate buffer (*p*H 7.4, $\frac{1}{10}$ mol), 1 c.c. of KNO_3 solution ($\frac{1}{100}$ mol), 2 c. c. of leucomethylene blue ($\frac{1}{50}$ mol), and 1 c.c. of inhibitor solution or distilled water. The tube was incubated for 1 hour at 37° and the nitrite thus formed was determined.

Determination of nitrite: The reaction mixture was decolorized by activated charcoal and proteins were removed. Then Griess-Ilosvay's reagent was added and the pink color thus developed was determined colorimetrically with Pulfrich's stufenphotometer.

Effects of Inhibitors. In order to elucidate the chemical nature of nitrate reductase, we have studied the effects of some typical respiratory inhibitors on the action of this enzyme. The results of this experiment are summarized in Table 1.

Table 1.

Inhibitors.....	KCN			NaN_3		CO		monoiodo-acetic acid		cysteine	cystine
Concentrations.... (mol/l.)	10^{-4}	10^{-3}	10^{-2}	10^{-3}	10^{-2}	1 atm. (dark)	1 atm.* (light)	10^{-3}	10^{-2}	2×10^{-2}	2×10^{-2}
Degrees of in-.... hibition (%)	7	97	100	56	100	42	0	52	93	92	7

* The tube was illuminated by 100 watt lamp from a distance of 30 cm.

As is shown in Table 1, nitrate reductase is markedly inhibited by so-called "heavy metal reagents" such as KCN, NaN_3 and CO. This fact strongly suggests that a certain heavy metal is related to the activity of this enzyme. In fact Quastel[5] already assumed the participation of iron in the bacterial reduction of nitrate on the basis of his observation with resting bacteria. Our experiment with cell-free enzyme also indicates in accordance with his assumption that the heavy metal contained in nitrate reductase must be iron, because we have shown, as is recorded in Table 1, that CO-inhibition of nitrate reductase completely disappears by light and it is well known that among CO-compounds of various heavy metals and their complexes, so far as examined, only those of iron and its complexes are photodissociable and therefore their catalytic activities, if any,

(5) J. H. Quastel, *Nature*, **130** (1932), 207; cf. H. Burström, *Planta*, **29** (1939), 292.

will be restored by light.

Although the above experiment is not sufficient to acquire an accurate knowledge about the rôle of iron in the process of enzymic reduction, it seems very attractive for us to consider that the essential function of the iron consists in an alternative cycle of valency between ferric and ferrous states, since nitrate reductase is inhibited both by KCN and CO; the former combines with ferric iron in almost all cases and the latter solely with ferrous iron.

In addition it must be noticed that this enzyme is intensively inhibited by a low concentration of monoiodoacetic acid, a specific inhibitor for sulfhydryl enzyme. Cysteine is also poisonous, but cystine is almost without effect. These facts feem to show that the sulfhydryl (−SH) or disufide (−S−S−) group may be connected with the activity in some manner.

Spectroscopic Observations. The crude preparation of nitrate reductase obtained by our method shows a brownish yellow color in a concentrated aqueous solution. This solution, when reduced by $Na_2S_2O_4$, exhibits three absorption bands in the visible region under Zeiss microspectrometer. The non-reduced solution shows only very weak and diffused absorptions (oxidized bands). The positions of the three reduced bands are as follows:

(1) 585 mμ, very weak and diffused.
(2) 560 mμ, intense and sharp.
(3) 530 mμ, weak and sharp.

Among these bands, (2) and (3) are apparently identical with the α- and β-bands of cytochrome b which were observed by Keilin[6] with Bac. coli suspension. In contrast with (2) band (3), band (1) is very weak and diffused, the origin of which is yet unknown.

In order to decide whether there exists any relationship between nitrate reductase and these bands, the following experiments have been carried out. The enzyme solution was precipitated fractionally into five portions by acetone (below 0°) and the activity of nitrate reductase and intensities of the reduced bands were determined. The results are shown in Table 2.

Table 2.

Fractions	Volume % of acetone when precipitated	Relative activities of nitrate reductase	Intensities of the band at 585 mμ	Intensities of the bands at 560 and 530 mμ
I	0 −33.3	100	+	+++
II	33.3−50	15	+	+
III	50 −66.6	4	++	±
IV	66.6−75	0	−	−
V	75 −83.3	0	−	−

Further addition of acetone produced no precipitate.

(6) D. Keilin, *Ergeb. Enzymforsch.*, 2 (1933), 239.

The following facts have been made clear by these results: (1) the band at 585 mμ has no relation to nitrate reductase, and (2) the intensities of the bands at 560 mμ and 530 mμ, which are regarded as the reduced bands of cytochrome b, are apparently parallel with the activity of this enzyme. This parallelism seems to be an evidence, though not decisive, of the identity of cytochrome b with nitrate reductase. That nitrate reductase may contain iron as an essential component (as postulated by our inhibition studies) also agrees with this assumption, for cytochrome b is an iron-porphyrin enzyme.

We have further attempted some experiments to ascertain the identity of these two substances. If our assumption is correct and nitrate reductase (= cytochrome b) undergoes cyclic oxidation and reduction, the process of enzymic reduction of nitrate may be shown by the following scheme.

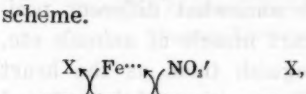

X, XH_2....oxidized and reduced forms of intermediary hydrogen carrier.
Fe···, Fe··....oxidized and reduced forms of nitrate reductase (cytochrome b)

From this scheme it is expected that the reduced bands of cytochrome b will shift to the oxized bands when nitrate is added. We found, contrary to our expectation, that no change occurs in the absorption bands of cytochrome b, previously reduced by $Na_2S_2O_4$, even when a large amount of nitrate was added. This fact is not, however, contradictory with our assumption, since we later found that the enzyme treated with $Na_2S_2O_4$ loses its activity irreversibly. To avoid the use of $Na_2S_2O_4$ we then adopted the following method. In the main room of a Thunberg tube 3 c.c. of enzyme solution, 0.5 c.c. of sodium formate (1 mol), and 0.5 c.c. of methylene blue (1:10,000) were put in. In the side chamber of the tube was placed 0.5 c.c. of KNO_3 (2 mol). Then the tube was evacuated and incubated at 37°. As our enzyme preparation contains powerful formic dehydrogenase as well as nitrate reductase the methylene blue was soon decolorized and simultaneously the reduced bands of cytochrome b appeared. After complete decolorization of methylene blue KNO_3 was mixed with the enzyme solution. Then immediately decrease of the intensities of the bands of reduced cytochrome b was observed and they approached those of oxidized form. But this conversion ceased incompletely probably due to an establishment of an equilibrium between the oxidizing power of nitrate and the reducing tendency of formic dehydrogenase system. This result seems to support our assumption firmly.

It is quite natural to expect then that some changes will take place by KCN and NaN_3 in the absorption bands of cytochrome b, since these reagents inhibit nitrate reductase markedly. But we could not observe any change of absorption spectrum by KCN and NaN_3 in either the

oxidized or reduced enzyme solution. Reduced cytochrome b has not only α- and β-bands, but also γ-band at about 430 mμ which can not be observed by this method. As the possibility still remains that γ-band will be affected by these inhibitors, we will study this point in future.

Discussion. Although many problems are still left unsolved about the chemical nature of nitrate reductase, the identity of this enzyme with cytochrome b becomes quite probable by our present investigations.

Cytochrome b is widely distributed in aerobic cells and is considered as an important factor of aerobic cell respiration, but studies on this substance have been neglected compared with other components of the cytochrome system. Up to the present it has been investigated mainly by spectroscopic method and it is now confirmed that there are two kinds of cytochrome b whose absorption bands lie at somewhat different positions. As one of them is present in the heart muscle of animals etc. and the other in Bac. coli, etc., we will distinguish them as the heart muscle type and Bac. coli types respectively. The positions of the reduced bands are as follows:

	α-band	β-band
Heart muscle type	564 mμ	534 mμ
Bac. coli type	460 mμ	630 mμ

To which component of cytochrome b must be attributed the activity of nitrate reductase? We assume that cytochrome b of Bac. coli type is the very nature of nitrate reductase and that of the heart muscle type is unconcerned with this enzyme. This assumption also answers the question why there are tissues and cells which can not reduce nitrate in spite of a high content of cytochrome b.

We have further clarified by consulting "Bergey's Manual of Determinative Bacteriology"[7] and Tamiya and Yamagutchi's[8] list on cytochrome types of microorganisms that (1) bacteria without cytochromes can not reduce nitrate at all, (2) almost all organisms containing cytochrome b of Bac. coli type can reduce nitrate, but those of the heart muscle type are not able to reduce nitrate except in a few cases. Moreover Bernheim and Dixon[9] reported that among various tissues of many animals only the liver (and also the muscle of a few species) can reduce nitrate, while according to Yoshikawa[10], cytochrome b of the liver is Bac. coli type. This parallelism between the ability of nitrate reduction and the existence

(7) D. H. Bergey, "Bergey's Manual of Determinative Bacteriology", 4th Ed., Baltimore (1934).

(8) H. Tamiya and S. Yamagutchi, *Acta Phytochimica*, **6** (1934), 105.

(9) F. Bernheim and M. Dixon, *Biochem. J.* **22** (1928), 125.

(10) H. Yoshikawa, from discussions at the 1st "Symposium on Enzyme Chemistry" held at Tokyo in October, 1948.

of Bac. coli type cytochrome b also seems to be favourable for our assumption.

Summary.

The effects of various inhibitors on nitrate reductase have been investigated and some spectroscopic observations have been made to elucidate the chemical nature of nitrate reductase. From these studies it becomes very probable that cytochrome b of Bac. coli type is identical with nitrate reductase.

The authors express their sincere thanks to Prof. H. Tamiya for his kind suggestion to the present studies, and also to Prof. S. Hosoya for his kindness in granting many conveniences for these experiments.

Chemical Institute, Faculty of Science,
Nagoya University.